

AD-A053 294

WESTINGHOUSE DEFENSE AND ELECTRONIC SYSTEMS CENTER B--ETC F/G 1/5
STUDY OF ROUGH GROUND AND GRADING CRITERIA FOR INSTRUMENT LANDI--ETC(U)
MAR 78 J T GODFREY, H F HARTLEY, R A MOORE DOT-FA74WA-3353
FAA-RD-78-42 NL

UNCLASSIFIED

1 of 1
AD
A053294



END
DATE
FILMED
6-78
DDC

Report No. **FAA-RD-78-42**

12

STUDY OF ROUGH GROUND AND GRADING CRITERIA FOR INSTRUMENT LANDING SYSTEM GLIDE SLOPE SITE PREPARATION

AD A 053294

J. T. Godfrey
H. F. Hartley
R. A. Moore
G. J. Moussally

D87-FA 74WA-3353



1269p.

DDC

RECEIVED
APR 27 1978
RECEIVED

AD No. **DDC FILE COPY**

MAR 1978

INTERIM REPORT

Document is available to the U.S. public through the National Technical Information Service, Springfield, Virginia 22161.

Prepared for

**U.S. DEPARTMENT OF TRANSPORTATION
FEDERAL AVIATION ADMINISTRATION
Systems Research & Development Service
Washington, D.C. 20590**

405-532

B

NOTICE

This document is disseminated under the sponsorship of the Department of Transportation in the interest of information exchange. The United States Government assumes no liability for its contents or use thereof.

Technical Report Documentation Page

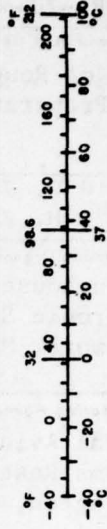
1. Report No. FAA-RD-78-42		2. Government Accession No.		3. Recipient's Catalog No.	
4. Title and Subtitle Study of Rough Ground and Grading Criteria for ILS GS Site Preparation				5. Report Date March 1978	
				6. Performing Organization Code	
7. Author(s) G. J. Moussally, R. A. Moore, J. T. Godfrey, H. F. Hartley				8. Performing Organization Report No.	
9. Performing Organization Name and Address Westinghouse Defense and Electronic Systems Center Electronic Systems Division Baltimore, Maryland 21203 <i>use 405532 TB</i>				10. Work Unit No. (TRAI5)	
				11. Contract or Grant No. DOT-FA74WA-3353 <i>NW</i>	
12. Sponsoring Agency Name and Address Federal Aviation Administration Systems Research and Development Service Washington, D.C. 20591				13. Type of Report and Period Covered Interim Report Modification #5	
				14. Sponsoring Agency Code ARD-700	
15. Supplementary Notes					
16. Abstract <p>The scattering of electromagnetic radiation from rough surfaces has been studied. The diffuse and specular components of the scattered field are treated separately. Current grading of ILS sites requires rather stringent preparation of the ground. The application of this report is to develop grading criteria that reflect the statistical nature of the disturbance in observed signal rather than simply to consider the maximum allowable phase differences as the basis for establishing a grading criteria. ↗</p>					
17. Key Words Instrument Landing Systems Glide Slope Scattering Site Preparation Rough Ground			18. Distribution Statement Document is available to the U.S. public through the National Technical Information Service, Springfield, Virginia 22161.		
19. Security Classif. (of this report) UNCLASSIFIED		20. Security Classif. (of this page) UNCLASSIFIED		21. No. of Pages 61	22. Price

METRIC CONVERSION FACTORS

Approximate Conversions to Metric Measures

Symbol	When You Know	Multiply by	To Find	Symbol
	LENGTH			
in	inches	2.5	centimeters	cm
ft	feet	30	centimeters	cm
yd	yards	0.9	meters	m
mi	miles	1.6	kilometers	km
	AREA			
in ²	square inches	6.5	square centimeters	cm ²
ft ²	square feet	0.09	square meters	m ²
yd ²	square yards	0.8	square meters	m ²
mi ²	square miles	2.6	square kilometers	km ²
	acres	0.4	hectares	ha
	MASS (weight)			
oz	ounces	28	grams	g
lb	pounds	0.45	kilograms	kg
	short tons (2000 lb)	0.9	tonnes	t
	VOLUME			
tsp	teaspoons	5	milliliters	ml
Tbsp	tablespoons	15	milliliters	ml
fl oz	fluid ounces	30	milliliters	ml
c	cups	0.24	liters	l
pt	pints	0.47	liters	l
qt	quarts	0.95	liters	l
gal	gallons	3.8	liters	l
ft ³	cubic feet	0.03	cubic meters	m ³
yd ³	cubic yards	0.76	cubic meters	m ³
	TEMPERATURE (exact)			
°F	Fahrenheit temperature	5/9 (after subtracting 32)	Celsius temperature	°C

Symbol	When You Know	Multiply by	To Find	Symbol
	LENGTH			
mm	millimeters	0.04	inches	in
cm	centimeters	0.4	inches	in
m	meters	3.3	feet	ft
m	meters	1.1	yards	yd
km	kilometers	0.6	miles	mi
	AREA			
cm ²	square centimeters	0.16	square inches	in ²
m ²	square meters	1.2	square yards	yd ²
km ²	square kilometers	0.4	square miles	mi ²
ha	hectares (10,000 m ²)	2.5	acres	ac
	MASS (weight)			
g	grams	0.005	ounces	oz
kg	kilograms	2.2	pounds	lb
t	tonnes (1000 kg)	1.1	short tons	st
	VOLUME			
ml	milliliters	0.03	fluid ounces	fl oz
l	liters	2.1	pints	pt
l	liters	1.06	quarts	qt
l	liters	0.26	gallons	gal
m ³	cubic meters	35	cubic feet	ft ³
m ³	cubic meters	1.3	cubic yards	yd ³
	TEMPERATURE (exact)			
°C	Celsius temperature	9/5 (then add 32)	Fahrenheit temperature	°F



*1 in ± 2.54 (exact). For other exact conversions and more detailed tables, see NBS Misc. Publ. 286, Units of Weights and Measures, Price \$2.25, SD Catalog No. C13.10-286.

TABLE OF CONTENTS

	<u>Page</u>
1. INTRODUCTION	3
2. SPECULAR CONTRIBUTION OF SCATTERED FIELD	5
3. THE DIFFUSE CONTRIBUTION TO THE SCATTERED FIELD	9
4. CALCULATION OF DDM	11
5. CALCULATION OF CORRELATION DISTANCES	16
6. NUMERICAL RESULTS FOR GRADING CRITERIA	18
7. DISCUSSION	21

ACCESSION for	
NTIS	White Section <input checked="" type="checkbox"/>
DDC	Buff Section <input type="checkbox"/>
UNANNOUNCED	<input type="checkbox"/>
JUSTIFICATION _____	
BY _____	
DISTRIBUTION/AVAILABILITY CODES	
Dist.	AVAIL and/or SPECIAL
A	

LIST OF ILLUSTRATIONS

<u>Figure</u>		<u>Page</u>
II-2	Illustration of Areas Involved in Determining Grading Criteria	1
II-A1	Distribution of Heights, Δh , and Illustration of σ	2
II-1	Definition of Coordinate Systems Illustrating Space and Local Coordinate Geometries	24
II-3a	Diffuse DDM Error vs Roughness, Capture Effect, 30,000 ft	25
II-3b	Diffuse DDM Error vs Roughness, Capture Effect, 15,000 ft	26
II-3c	Diffuse DDM Error vs Roughness, Capture Effect, 10,000 ft	27
II-3d	Diffuse DDM Error vs Roughness, Capture Effect, 5,000 ft	28
II-3e	Diffuse DDM Error vs Roughness, Capture Effect, 3,000 ft	29
II-4a	Diffuse DDM Error vs Roughness, Null Reference, 30,000 ft	30
II-4b	Diffuse DDM Error vs Roughness, Null Reference, 15,000 ft	31
II-4c	Diffuse DDM Error vs Roughness, Null Reference, 10,000 ft	32
II-4d	Diffuse DDM Error vs Roughness, Null Reference, 5,000 ft	33
II-4e	Diffuse DDM Error vs Roughness, Null Reference, 3,000 ft	34
II-5a	Diffuse DDM Error vs Roughness, Sideband Reference, 3,000 ft	35
II-5b	Diffuse DDM Error vs Roughness, Sideband Reference, 15,000 ft	36

<u>Figure</u>		<u>Page</u>
II-5c	Diffuse DDM Error vs Roughness, Sideband Reference, 10, 000 ft	37
II-5d	Diffuse DDM Error vs Roughness, Sideband Reference, 5, 000 ft	38
II-5e	Diffuse DDM Error vs Roughness, Sideband Reference, 3, 000 ft	39
II-6a	Specular DDM Error vs Roughness, Capture Effect, 30, 000 ft	40
II-6b	Specular DDM Error vs Roughness, Capture Effect, 15, 000 ft	41
II-6c	Specular DDM Error vs Roughness, Capture Effect, 10, 000 ft	42
II-6d	Specular DDM Error vs Roughness, Capture Effect, 5, 000 ft	43
II-6e	Specular DDM Error vs Roughness, Capture Effect, 3, 000 ft	44
II-7a	Specular DDM Error vs Roughness, Null Reference, 30, 000 ft	45
II-7b	Specular DDM Error vs Roughness, Null Reference, 15, 000 ft	46
II-7c	Specular DDM Error vs Roughness, Null Reference, 10, 000 ft	47
II-7d	Specular DDM Error vs Roughness, Null Reference, 5, 000 ft	48
II-7e	Specular DDM Error vs Roughness, Null Reference, 3, 000 ft	49
II-8a	Specular DDM Error vs Roughness, Sideband Reference, 30, 000 ft	50
II-8b	Specular DDM Error vs Roughness, Sideband Reference, 15, 000 ft	51
II-8c	Specular DDM Error vs Roughness, Sideband Reference, 1, 000 ft	52
II-8d	Specular DDM Error vs Roughness, Sideband Reference, 5, 000 ft	53

<u>Figure</u>		<u>Page</u>
II-8e	Specular DDM Error vs Roughness, Sideband Reference, 3,000 ft	54
II-9	Capture Effect Fly-Ins Over Transverse Edge	55
II-10	Null Reference Fly-Ins Over Transverse Edge	56
II-11	Sideband Reference Fly-Ins Over Transverse Edge	57
II-12	Fractional Revised Grading Cost Based on Current Cost	58

LIST OF TABLES

<u>Table</u>		<u>Page</u>
II-1	Values of Roughness $\sigma_2(\lambda)$ vs $\sigma_1(\lambda)$ for Variance in DDM, ΔDDM^s	59
II-2	Values of Roughness $\sigma_D(\lambda)$ vs DDM Error from Diffuse Region	60
II-3	Radius of Diffuse Area vs $\sigma_1(\lambda)$	61

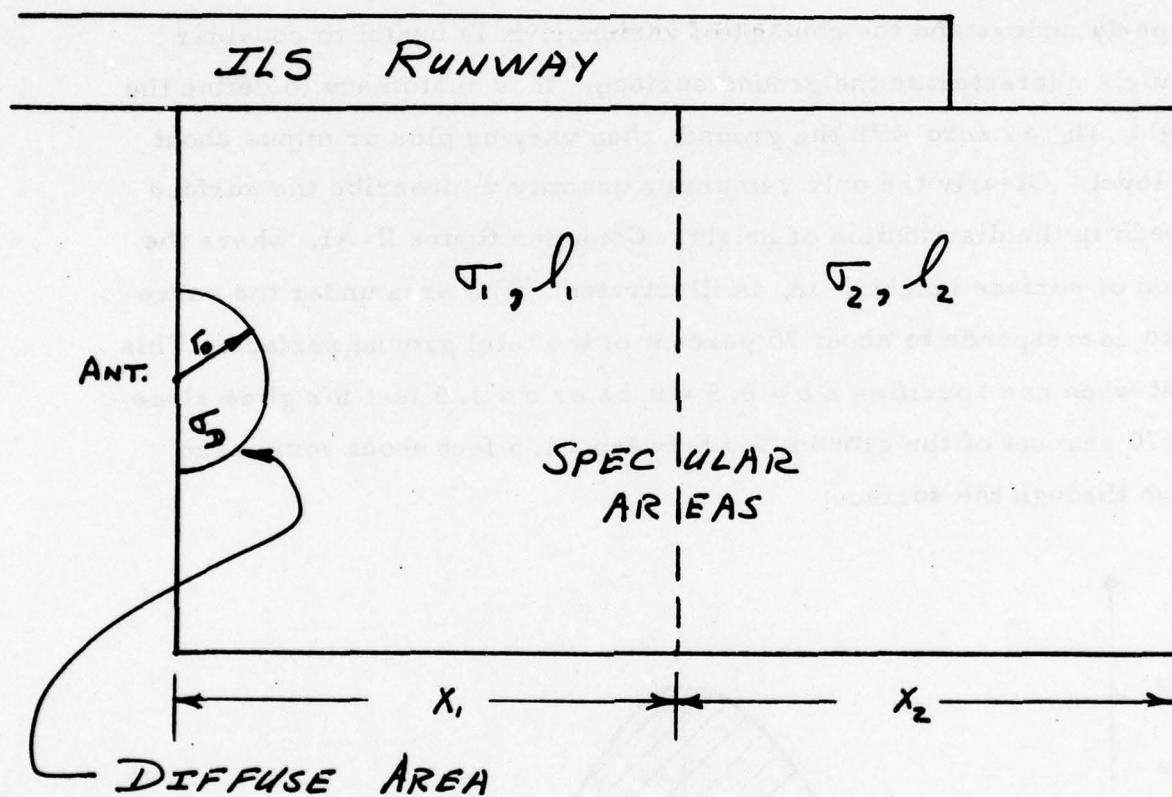


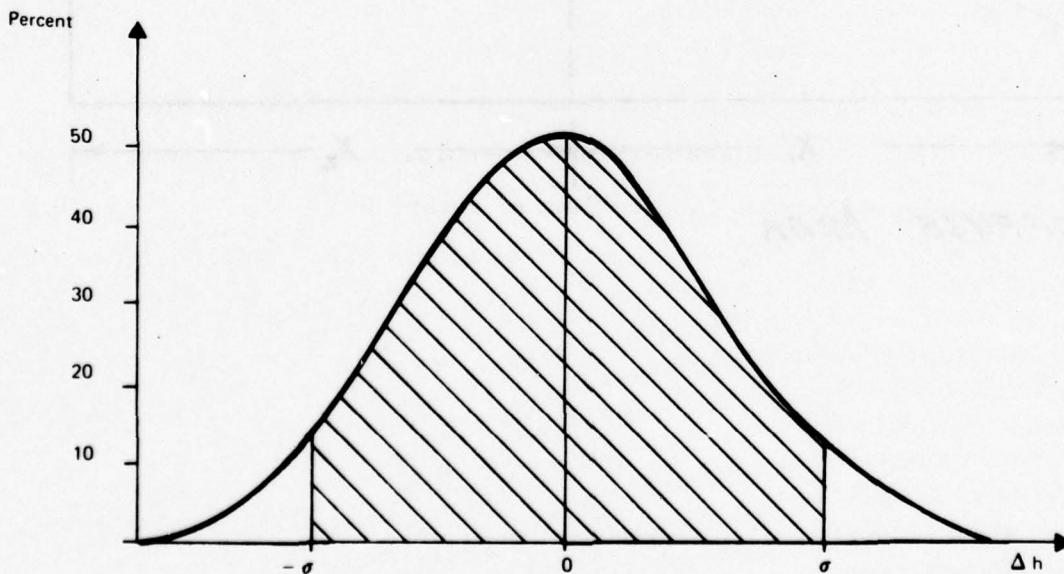
FIGURE II-2

ILLUSTRATION OF AREAS INVOLVED
IN DETERMINING GRADING CRITERIA

Discussion of σ_1 , σ_2 , and σ_D

Throughout the presentation of this report, the quantities σ_1 , σ_2 , and σ_{DD} are used to characterize the ground surface. The units of these variances are wavelengths, with one wavelength (λ) for glide slope analysis corresponding to approximately 3 feet. Therefore, a value of $\sigma = 0.5 = 0.5\lambda$ translates as $\sigma = 1.5$ feet.

To properly understand the concept of variance, it is useful to consider how one might characterize the ground surface. It is customary to define the mean height, Δh , as zero with the ground, then varying plus or minus about this zero level. Clearly the only remaining quantity to describe the surface is the spread in the distribution of height. Consider figure II-A1, where the distribution of surface heights, Δh , is illustrated. The area under the curve between $\pm\sigma$ corresponds to about 70 percent of the total ground surface. This means that when one specifies a $\sigma = 0.5 = 0.5\lambda$ or $\sigma = 1.5$ feet for glide slope systems, 70 percent of the ground lies between ± 1.5 feet about some zero level drawn through the surface.



77-1019-V-1

Figure II-A1 Distribution of Heights, Δh , and Illustration of σ

1. INTRODUCTION

Scattering of electromagnetic waves from rough surfaces has been studied through the Kirchoff approach¹ for very rough surfaces, the small perturbation method of Rice² for slightly rough surfaces, and the composite model^{3, 4, 5} for surfaces with both small and large undulations. * Surfaces characterized by more than one statistically distributed roughness have been discussed by Beckmann.⁶ The approach used in the present work is discussed by Weiss⁷ and consists of treating the specular and diffuse components of the scattered field separately. The diffuse scattered radiation is modeled on the basis of subdividing the relevant scattering area into small rectangular blocks and using the plane wave approximation to get the scattered fields. For the specular portion of the radiation, the half-plane solutions of Senior,⁸ Woods,⁹ and Bromwich¹⁰ are modified to yield expressions for scattering from slightly rough half-planes. The results are very similar to the conventional Rayleigh result for specular scatter (reference 7, p. 5).

Once expressions for the scattering of specular and diffuse radiations are obtained, they are applied to the problem of determining allowable grading for instrument landing systems. Current grading of ILS sites requires rather stringent preparation of the ground, and the application of this paper is to develop grading criteria that reflect the statistical nature of the disturbance in observed signal rather than simply to consider the maximum allowable phase differences as the basis for grading criteria, as is now done.

The results of this work as will be seen, indicate that the current grading is too stringent and that substantial cost savings can be effected through a

*Numbered references appear at the end of this document.

more systematic approach. In specifying the grading criteria, the expressions developed allow for the treatment of several statistically different surfaces with the requirement that the solutions be self-consistent when the roughness of each adjacent surface is equal.

2. SPECULAR CONTRIBUTION OF SCATTERED FIELD

In developing expressions for the field scattered from a slightly rough half-plane, it is appropriate to consider the two-dimensional dual-integral formulation of the problem¹¹ and then generalize to the three-dimensional case as outlined by Senior. Consider the plane electromagnetic wave with harmonic time dependence $\exp(i\omega t)$ incident obliquely at an angle α_0 on a slightly rough half-plane, $z = \Delta h(x, y)$, and $x \leq x_e$, where $\langle \Delta h \rangle = 0$ as illustrated in figure II-1. If XYZ defines a set of space axes with unit vectors \hat{i} , \hat{j} , and \hat{k} , a local coordinate system on the surface can be defined with axes X'Y'Z' and unit vectors \hat{i}' , \hat{j}' , and \hat{k}' respectively. For slightly rough ground, the variation of $\Delta h(x, y)$ with x and y is small compared to unity, and if the variation in y is small compared to x , the surface unit vectors are related to the space unit vectors through

$$\hat{i}' = \hat{i} + \Delta h_x \hat{k} \quad (1a)$$

$$\hat{j}' = \hat{j} \quad (1b)$$

$$\hat{k}' = -\hat{i} \Delta h_x + \hat{k} \quad (1c)$$

where $\Delta h_x = \partial \Delta h / \partial x$. The incident plane wave satisfies

$$\begin{aligned} e^{-ikz} &= e^{-ik(x \cos \alpha_0 - z \sin \alpha_0)} \\ &= e^{-ik(x(\cos \alpha_0' + \Delta h_x \sin \alpha_0') - (z - \Delta h)(\sin \alpha_0' - \Delta h_x \cos \alpha_0'))} \end{aligned} \quad (2)$$

where α_0' is the incident angle defined relative to the surface local coordinate system. The dual integral equations describing the scattered fields at a point on the local surface ($z = \Delta h$) because

$$\int_0^\infty \frac{P(\mu')}{\sqrt{1-\mu'^2}} e^{ik(x_e - x')(\mu' - \Delta h_x \sqrt{1-\mu'^2})} d\mu' = -e^{ik(x_e - x')(\mu_0' + \Delta h_x \sqrt{1-\mu_0'^2})} \quad (3a)$$

$$\int_{-\infty}^{\infty} P(\mu') e^{ik(x_e - x')(\mu' - \Delta h_x \sqrt{1 - \mu'^2})} d\mu' = 0 \quad (x > x_e) \quad (3b)$$

where $\mu' = \cos \alpha'$, $\mu'_0 = \cos \alpha'_0$ and $P(\mu')$ is an appropriate Fourier weighting coefficient defined by (see reference 1, p. 567)

$$P(\mu') = \frac{i}{2\pi} \frac{\sqrt{1 - \mu'_0} \sqrt{1 - \mu'}}{\mu' + \mu'_0} \quad (4)$$

Equations (3a) and (3b) can be further simplified if the variations across the surface are characterized by large correlation distances (small Δh_x). Here the slope terms can be ignored and the scattered field simply becomes that for the usual half-plane solutions with z replaced by $z - \Delta h$ (see reference 11, p. 567). Generalizing the two-dimensional solution to three dimensions as outlined by Senior (reference 8), the scattered Y-component of the field from a dipole along the Y-axis becomes

$$\begin{aligned} \epsilon_{YY}^S(\Delta h) = & -\frac{k^2}{2\pi} \int d\alpha \int d\beta \int d\gamma \frac{\sin(1/2)\alpha \sin(1/2)\gamma}{\cos\alpha + \cos\gamma} \\ & \cdot e^{-ik[(x_e - x_0)\cos\alpha \cos\beta + (z_0 - \Delta h)\sin\alpha \cos\beta - y_0 \sin\beta]} \\ & \cdot e^{ik[(x_e - x)\cos\gamma \cos\beta + (z - \Delta h)\sin\gamma \cos\beta + y \sin\beta]} \end{aligned} \quad (5)$$

where the integrals over α , β , and γ are the steepest descent paths of reference 2; x_0 , y_0 , z_0 denotes the position of the dipole; x , y , z denotes the observer point; and x_e denotes the position of the half-plane edge. The notation for the field in equation (5) corresponds to a scattered field ϵ_{ij}^S , where i denotes the field component in space and j denotes the axis along which the dipole is parallel.¹² The dependence of the specular scattered field integrals on the reflection coefficient for horizontally polarized radiation, $R_0^-(\alpha)$, has been avoided since, to a good approximation for horizontally polarized radiation scattered off a plane earth,¹³

$$|R_0^-(\alpha)| \doteq 1 \quad (0 \leq \alpha \leq 4^\circ) \quad (6)$$

where the bulk of the contribution to the integrals comes from the specular angle with $\alpha < 4^\circ$ ($\lambda = 3$ m). For glide slope arrays, the dipole is parallel to the Y-space axis with the aircraft antenna similarly polarized so that the field component, C_{YY}^S , is the case of interest.

Expanding the exponentials in Δh and reducing the integrals of equation (5) to Fresnel integrals in the manner outlined by Senior,

$$C_{YY}^S(\Delta h) = \sum_{mn}^{\infty} (-1)^{m+n} \frac{\Delta h^{m+n}}{m!n!} \left(\frac{\partial}{\partial Z}\right)^m \left(\frac{\partial}{\partial Z}\right)^n I_{YY}^S \quad (7)$$

where

$$I_{YY}^S = k \left[\text{sgn}(\tau_S) G_S(|\tau_S|) - \text{sgn}(\tau_R) G_R(|\tau_R|) \right] \quad (8)$$

and where $k = 2\pi/\lambda$

$$C_u(|\tau_u|) = \sqrt{\frac{2}{\pi}} e^{i\pi/4} \frac{e^{-iku}}{\sqrt{R_1(R_1+u)}} F(|\tau_u|) \quad (9a)$$

$$F(|\tau_u|) = \int_{|\tau_u|}^{\infty} e^{-i\tau^2} d\tau \quad (9b)$$

where $u = R$ or S and

$$\tau_u = 2\sqrt{\frac{kRr_0}{R_1+u}} \cos(\theta \pm \theta_0)/2 \quad (10a)$$

$$u = \left[(x-x_0)^2 + (y-y_0)^2 + (z \pm z_0)^2 \right]^{1/2} \quad (10b)$$

In equations (10a) and (10b) the plus sign corresponds to $u = S$ and the minus sign to $u = R$. The angles θ and θ_0 are defined by $z = r \sin \theta$, $x-x_e = r \cos \theta$ ($x > x_e$), $z_0 = r_0 \sin \theta_0$, and $x_e - x_0 = r_0 \cos \theta_0$ ($x_e > x_0$). The remaining variables are

$$r = [(x-x_e)^2 + z^2]^{1/2} \quad (11a)$$

$$r_o = [(x_o-x_e)^2 - z_o^2]^{1/2} \quad (11b)$$

$$R_1 = [(r+r_o)^2 + (y-y_o)^2]^{1/2} \quad (11c)$$

The solutions to the specular scattered field presented in equation (7) is equivalent to the Rayleigh (see reference 5, p. 240) result for rough scatter except that it has been developed for a slightly rough half-plane. This solution is quite adequate for treatment of glide slope problems where the specular angles are always small ($\leq 4^\circ$).¹⁴ It was found that, for ground roughness with variances $\sigma \leq 1.7\lambda$ (assuming normally distributed ground), a second-order expansion in equation (7) is sufficient.

3. THE DIFFUSE CONTRIBUTION TO THE SCATTERED FIELDS

The diffuse scattering contribution to the fields is not easily determined from theoretical considerations. In general this contribution is linearly independent of the specular scattered fields and can be written in the form (for the Y-component from a dipole along the Y-axis)

$$\epsilon_{YY}^{\text{DIF}} \int_S R_o^-(\alpha) \rho_D(\alpha) E_{YY}^{\text{DIF}}(a) da, \quad (12)$$

where $\alpha = \alpha(a)$ is the incident angle measured from the surface to the incident wave vector, R_o^- is the reflection coefficient, and ρ_D is the diffuse scattering coefficient. The reflection coefficient, R_o^- , is that for horizontally polarized radiation, and since the integral in equation (12) includes angles where R_o^- is appreciably different from unity, it must be included in the expression for diffuse scatter. The functional behavior of $R_o^-(\alpha)$ was obtained from Beckman and Spizzichino (reference 13, p. 220) as was the behavior of $\rho_D(\alpha)$ (reference 13, p. 340). The diffuse scattering coefficient functionally depends on the parameter

$$\xi = \frac{4\sigma_D \sin \alpha}{\lambda} \quad (13)$$

where σ_D is the variance of the roughness.

The integral appearing in equation (12) was evaluated numerically assuming the surface to be subdivided into small rectangles subject to the condition that the incident radiation could be approximated as a plane wave over each small rectangle. This criterion was used to determine the appropriate size of each rectangular subsection of the surface. The scattered field due to each rectangular section was calculated within the framework of the vector Kirchoff integral representation of diffracted radiation, with the result

$$E_{YY}^{DIF}(a) = -\frac{ik}{2\pi} \frac{e^{ikr}}{r_s r_A} e^{ik(r_s + r_A)} a_1 a_2 \frac{\sin A}{A} \frac{\sin B}{B} \quad (14)$$

$$\left[\hat{k}_2 \times (\hat{k}_2 \times (\hat{h} \times (\hat{j} \times \hat{u}_1))) \right]_j$$

where \hat{j} is the direction of the dipole and measured scattered polarization, \hat{k}_2 is the unit scattered wave vector, \hat{h} is a unit vector normal to the surface element, R is as defined by equation (10b), r_s is the distance from the plate center to the source, r is the distance from the plate center to the observer, a_1 and a_2 are the length and width of the rectangular section, and

$$A = k \cos(\beta/2) \sin\theta \cos\phi a_1$$

$$B = k \cos(\beta/2) \sin\theta \sin\phi a_2$$

$$\beta = \text{angle between } \hat{j} \text{ and } \hat{k}_2$$

where θ and ϕ are spherical coordinates defining the direction of a vector \hat{k}_3 in the plane of \hat{j} and \hat{k}_2 that bisects the angle β . The limits on the surface of integration, S , of equation (12) were taken as that value of ξ such that P_D was ≤ 0.01 .

4. CALCULATION OF DDM

If p defines the position of the observer ($p(x, y, z)$) and $p'(m)$ defines the position of the m th dipole in the radiating array, the difference in depth of modulation (DDM) signal (see reference 12) is defined by

$$\text{DDM}(p) = NR e \frac{\sum_1^n d_m^{\text{SBO}} E_{YY}(p, p'(m))}{\sum_1^n d_m^{\text{CSB}} E_{YY}(p, p'(m))} \quad (15)$$

where N is an appropriate normalization, d_m^{SBO} is the dipole amplitude and phase of the m th dipole radiating the sideband signal, and d_m^{CSB} is the dipole amplitude and phase of the m th dipole radiating the carrier signal. The complex field, E_{YY} , contains both the scattered and direct radiation. The normalization, N , is obtained by requiring the DDM to be $\pm 75 \mu\text{A}$ at angles of $\pm 0.35^\circ$ about the desired aircraft glidepath.

Contributions to the DDM from the diffuse and specular radiation are statistically uncorrelated; consequently, it is useful to treat each type of radiation separately, with the requirement that the total DDM (being the sum for uncorrelated components) be less than a prescribed amount that is based on the tolerances allowed for DDM deviations.¹⁵ The total diffuse field becomes

$$E_{YY}^D = k^2 \left(\frac{e^{-ikR}}{kR} - \frac{e^{-ikS}}{kS} \right) + \epsilon_{YY}^{\text{DIF}} \quad (16)$$

which yields for the diffuse component of the DDM

$$\text{DDM}(p)^D = NR_e \frac{\sum_m^n d_m^{\text{SBO}} E_{YY}^D(p, p'(m))}{\sum_m^n d_m^{\text{CSB}} E_{YY}^D(p, p'(m))} \quad (17)$$

The average over roughness in the diffuse component is implicitly contained in the expression for ρ_D where the dependence is expressed in terms of the variance σ_D .

Evaluation of the contribution to the specular component of the DDM requires, however, that the signal be averaged over the roughness function $\Delta h = \Delta h(x, y)$. In addition to finding the average DDM^S (specular contribution), it is necessary to examine the variance in specular DDM^S , $\sigma_{\text{DDM}^S}^S$, since this quantity is a measure of the spread of the specular component and, consequently, it represents the true measure of the deviation about the mean of the specular component. The distinction between the two procedures for calculating the components of DDM, DDM^D , and DDM^S is simplified if one recognizes that, while equation (17) represents a worst case calculation for the diffuse contribution owing to the fact that ρ_D implicitly contains the roughness already averaged, the expressions to be developed for $\sigma_{\text{DDM}^S}^S$ constitutes the worst case for specular DDM about the mean, $\langle \text{DDM}^S \rangle$.

In evaluating the average specular DDM, $\langle \text{DDM}^S \rangle$, and the variance, $\sigma_{\text{DDM}^S}^S$, it is desirable to introduce the bivariate distribution.¹⁶

$$f(\Delta h_i, \Delta h_j) = \frac{1}{2\pi\sigma_i\sigma_j\sqrt{1-\rho_{ij}^2}} \cdot \frac{1}{e^{-2(1-\rho_{ij}^2)}} \left[\left(\frac{h_i}{\sigma_i} \right)^2 + \left(\frac{h_j}{\sigma_j} \right)^2 - 2\rho_{ij} \left(\frac{h_i}{\sigma_i} \right) \left(\frac{h_j}{\sigma_j} \right) \right] \quad (18)$$

where σ_i and σ_j are the variances in height of $\Delta h_i = \Delta h(x_i, y_i)$ and $\Delta h_j = \Delta h(x_j, y_j)$. The correlation is measured by

$$\rho_{ij} = e^{-\left[\frac{\Delta h_i - \Delta h_j}{T}\right]^2} \quad (19)$$

For the cases considered here, it was found that ρ_{ij} was vanishingly small. It was found that the dependence of $\langle \text{DDM}^S \rangle$ and σ_{DDM}^S on the correlation coefficient was insignificant, and appropriate expressions for these quantities to the second order are

$$\begin{aligned} \langle \text{DDM}^S \rangle = NR e \left[\frac{a_0}{b_0} + \sigma_1^2 \left\{ \frac{1}{b_0} \sum_j a_{2j} + \frac{a_0}{(b_0)^3} \left[\sum_j (b_{1j})^2 - b_0 \sum_j b_{2j} \right] \right. \right. \\ \left. \left. - \frac{1}{(b_0)^2} \sum_j a_{1j} b_{1j} \right\} \right] \quad (20a) \end{aligned}$$

$$\sigma_{\text{DDM}}^S (\sigma_1)^2 = N^2 \left[(A_0)^2 + \sigma_1^2 \left\{ 2A_0 \sum_j A_2^j + \sum_j (A_1^j)^2 + 2A_0 \sum_j A_3^{jj} \right\} \right] - \langle \text{DDM}^S \rangle^2 \quad (20b)$$

where

$$a_0 = \sum_j^n d_j^{\text{SBO}} \cdot k^2 \left[\frac{e^{-ikR(j)}}{kR(j)} - \frac{e^{-ikS(j)}}{KS(j)} + I_{YY}^S(R(j), S(j)) \right] \quad (21a)$$

$$a_{1j} = d_j^{\text{SBO}} \cdot \left[2k^2 \frac{\partial}{\partial z} \frac{e^{-ikS(j)}}{KS(j)} - k^2 \left(\frac{\partial}{\partial z} + \frac{\partial}{\partial z_0} \right) I_{YY}^S(R(j), S(j)) \right] \quad (21b)$$

$$a_{2j} = d_j^{\text{SBO}} \cdot \left[-2k^2 \frac{\partial^2}{\partial z^2} \frac{e^{-ikS(j)}}{KS(j)} + \frac{k^2}{2} \left(\frac{\partial^2}{\partial z^2} + 2 \frac{\partial^2}{\partial z \partial z_0} \right) I_{YY}^S(R(j), S(j)) \right] \quad (21c)$$

with similar expressions for b_o , b_{1j} , and b_{2j} , where d_j^{SBO} is replaced by d_j^{CSB} . In equation (20b) the terms become

$$A_o = R_e \frac{a_o}{b_o} \quad (22a)$$

$$A_1^j = R_e \left(\frac{a_{1j}}{b_o} \right) - R_e \left(\frac{a_o b_{1j}}{(b_o)^2} \right) \quad (22b)$$

$$A_2^j = R_e \left(\frac{a_{2j}}{b_o} \right) - R_e \left(\frac{a_o b_{2j}}{(b_o)^2} \right) \quad (22c)$$

$$A_3^{jj} = R_e \left(\frac{a_o (b_{ij})^2}{(b_o)^3} \right) - \left(R_e \frac{a_{1j} b_{1j}}{(b_o)^2} \right) \quad (22d)$$

Grading criteria are based on subdividing the ground in front of the antenna into the three principal regions of figure II-2. A further development for the specular DDM is thus required; namely, it must provide for two areas characterized by different roughness, σ_1 , and σ_2 . Applying the principle of superposition to the half-plane solution described earlier, it is possible to characterize the ground of figure II-2 by a half-plane of width $(-\infty$ to $x_1)$ and a strip $(x_1$ to $x_2)$. Any expression for the resulting variance σ_{DDM}^S must be self-consistent in that when $\sigma_1 = \sigma_2$ the solution is the same as for a half-plane of width $(-\infty$ to $x_1 + x_2)$. Such a development can be obtained based on the earlier discussion with the result

$$\begin{aligned} [\sigma_{DDM}^S(\sigma_1, \sigma_2)]^2 = & N^2 \left[(C_o)^2 + \sum_j (C_{1j})^2 (\sigma_1^2 + \sigma_2^2) + \sigma_2^2 \sum_j (C_{ij})^2 \right. \\ & + 2 \sum_j C_{1j} C'_{1j} (\sigma_1 \sigma_2 p_{12}^2 - \sigma_2^2) - 2 \sum_j (C_{1j})^2 \sigma_1 \sigma_2 p_{12} \\ & + 2 C_o \left[\sum_j C'_{3jj} \sigma_2^2 + \sum_j C_{3jj} (\sigma_1^2 - \sigma_2^2) + \sum_j (C'_{2j} \sigma_2^2 \right. \\ & \left. + \sum_j C_{2j} (\sigma_1^2 - \sigma_2^2)) \right] - \langle DDM^S(\sigma_1, \sigma_2) \rangle^2 \end{aligned} \quad (23)$$

where

$$C_{1j} = R_e \left[\frac{a_{1j}}{b_o} - \frac{a_o}{(b_o)} b_{1j} \right] \quad x_e = x_1 \quad (24a)$$

$$C_{2j} = R_e \left[\frac{a_{2j}}{b_o} - \frac{a_o}{(b_o)^2} b_{2j} \right] \quad x_e = x_1 \quad (24b)$$

$$C_{3jj} = R_e \left[\frac{a_o}{(b_o)^3} b_{1j} b_{1j} - \frac{a_{1j} b_{1j}}{(b_o)^2} \right] \quad x_e = x_1 \quad (24c)$$

$$C_o = R_e \left[\frac{a_o}{b_o} \right] \quad x_e = x_2 \quad (24d)$$

Here the quantities C'_{1j} , C'_{2j} , and C'_{3jj} are defined in the same way as for the C 's appearing in equations (24), except that $x_e = x_2$. The correlation coefficient now becomes

$$P_{12} = e^{-\left[\frac{\sigma_1 - \sigma_2}{u} \right]^2} \quad (25)$$

It is clear that, when $\sigma_1 = \sigma_2$, equation (23) is self-consistent. An expression for $\langle \text{DDM}^S(\sigma_1, \sigma_2) \rangle$ is easily obtained from equation (20a).

5. CALCULATION OF CORRELATION DISTANCES

In figure 2 the areas characterized by σ_1 and σ_2 also included a dependence on the parameters l_1 and l_2 . The quantities, the correlation distances, specify the distance between peaks in the roughness and in general depend only on the statistical value of the ground (here assumed random). To simplify the calculation of roughness, it has been assumed that the slope terms appearing in equations (3a) and (3b) were ignored. Clearly, determination of an appropriate correlation distance should be consistent with this approximation.

Bareck⁷ has found that the density of specular points satisfies

$$n_A = \frac{7.255}{\pi^2 l^2} \exp \left\{ -\frac{\tan^2 \gamma}{s^2} \right\} \quad (26)$$

where

$$\tan \gamma = \frac{\sqrt{\sin^2 \theta_i - 2 \sin \theta_i \sin \theta_s \cos \theta_s + \sin^2 \theta_s}}{\cos \theta_i + \cos \theta_s} \quad (27)$$

with l being the correlation distance, $s^2 = 4\sigma^2/l^2$ is the mean slope at a point on the surface, θ_i is the incident angle, and θ_s is the scattered angle. The total number of specular points contained within an area satisfies

$$N_A = \int n_A dS. \quad (28)$$

Integration of equation (28) numerically yields the results for the first area (characterized by σ_1) that $N_A = 1$ when

$\frac{\sigma_1(\lambda)}{\lambda}$	$\frac{l(\lambda)}{\lambda}$	$\frac{\sigma_1}{l}$
0.1	2	0.05
0.2	3.5	0.057
0.3	5	0.06
0.4	6.5	0.06

Since for the small specular grazing angles appropriate to glide slope systems $N_A = 1$, it is clear that slopes of about 0.05 are required to satisfy the approximations used in this calculation. The values of $l(\lambda)$ above indicate how the ground correlations must be graded for various choices of σ_1 . A similar correlation for σ_2 with $N_A = 0.01$ yields slopes of 0.02. These criteria will be assumed when calculating the requirements on grading.

6. NUMERICAL RESULTS FOR GRADING CRITERIA

Figures II-3a, b, c, d, e illustrate the effect of the diffuse scattered field on the DDM for a standard earth and a surface infinite conductivity. These figures are for capture effect arrays and represent the error in DDM, DDM^D , compared with infinite ground results for range points at 30000, 15000, 10000, 5000, and 3000 feet from threshold. These points were chosen as representative of the flight path. The array is located 1100 feet behind threshold and 300 feet left of runway centerline. The worst derogation is seen to occur at 30000 feet from threshold. Table II-2 illustrates the relative values of $\sigma_D(\lambda)$ versus the error introduced into the DDM. It is clear, for example, that values of $\sigma_D = 0.032\lambda$ for metal surfaces and $\sigma_D = 0.044\lambda$ for standard earth correspond to errors on the order of 10 μA in the observed DDM for capture effect systems.

Figures II-4a, b, c, d, e and II-5a, b, c, d, e show similar plots for the null reference and sideband reference systems. Again the cases of a metal surface and standard earth are plotted. Table II-2 illustrates the range of values of σ_D for these systems versus maximum observed error in DDM. It is clear that the null reference system performs best with regard to ground roughness and diffuse scatter followed by the capture effect and sideband reference systems. This result is in keeping with the ground current structure near each array: The sideband reference has the highest, followed by the capture effect, and the null reference has the lowest ground currents near the antenna. Clearly, the higher the ground currents in the diffuse region, the greater the possibility for signal derogation due to diffuse scatter from rough ground. In addition, the standard earth case demonstrates substantially reduced error over a flat metal surface. The results

for the metal surface are qualitatively in agreement with the experimental observations of Lucas.¹⁸ Conventional grading of ILS sites is to within ± 0.1 foot during the first 1000 feet of an area.¹⁵ This would correspond to a surface roughness of about $\pm 0.03\lambda$, which indicates that the observed error due to diffuse scatter would be less than $2.5 \mu A$, $7.5 \mu A$, and $10 \mu A$ for null reference, capture effect, and sideband reference systems, respectively.

Figure II-2 shows a semicircular area of radius r_0 representing the region of dominant contribution to diffuse scatter. It is clear that r_0 is determined by the point at which $R_0^-(\alpha) \rho_D(\alpha)$ reach some minimum value so that the remaining contribution to diffuse scatter is negligible. Defining this point as the one at which 95 percent of the diffuse radiation is included in the expressions for diffuse field, one can specify a grading limit on the radius of this diffuse region as a function of the roughness σ_1 . Table II-3 illustrates the results for this radius versus σ_1 . As σ_1 increases, more diffuse scatter is observed coming from segments of the ground located further from the antenna, and, consequently, the amount of ground requiring grading to minimize diffuse scatter increases. It is important to note that, although the sideband reference has the highest ground currents near the antenna, they occur at closer distances to the array since the antenna elements are closer to the ground surface; consequently, a smaller segment of ground under this array is subject to diffuse scatter.

Figure II-6a, b, c, d, e, figure II-7a, b, c, d, e, and figure II-8a, b, c, d, e illustrate the specular contribution to the variance in the DDM versus σ_1 and σ_2 (the two roughness factors characterizing the areas in front of the arrays as shown in figure II-2). Several effects are clear from these figures. The contribution from the first area, σ_1 , dominates the behavior of the variance in DDM, and only at small and large distances from the array does the second area, characterized by σ_2 , introduce a significant effect. This is because, at small distances from the array, the edge of

the graded area that was taken to be 2000 feet noticeably degrades the pattern. This effect is illustrated in figures II-9, II-10, and II-11, where the influence of a truncated half-plane edge on the DDM is plotted for each system. At very large distances from threshold, substantial specular scatter occurs from the second region owing to the grazing angle of the reflected radiation, and one again expects σ_2 to become important.

Comparison of the behavior of the three systems demonstrates that the sideband reference performs most poorly, followed by the capture effect, with that followed closely by the null reference. This is in keeping with the fact that the dominant roughness effects come from the area closest to the array and that the ground currents are highest for the sideband reference, followed by the capture effect and null reference arrays in this area. It should be realized that the variance in the DDM is being plotted, and in effect this represents the allowable spread in DDM that could occur. (It accounts for the spread 99 percent of the time.)

Calculation of the probable limits of signal derogation must include the variance due to specular scatter, the change in the signal position about the infinite plane case (figures II-9, II-10, and II-11), and the contribution from the diffuse scatter. The area to be graded is illustrated in figure II-2, where the x-distances were determined by existing criteria and the y-distances were determined by the point at which lateral edges yield no substantial effect (see reference 12). The diffuse region is specified as in table II-2.

7. DISCUSSION

A technique for describing specular and diffuse scatter from slightly rough half-planes has been developed. The results are shown to be applicable to areas characterized by varying ground roughness statistics. Application of that technique for describing ground scatter to ILS sites demonstrates that the existing requirements on overall grading are presently too stringent.

The results for diffuse scatter indicate that current grading is sufficient to minimize the effects of such scatter and to yield patterns within current ILS glide slope requirements. The diffuse scatter results are in qualitative agreement with existing model range results and practical observations. The derogation due to specular scatter indicates that a substantial relaxation in grading is possible. Figure II-12 represents a typical cost-effectiveness plot versus σ_1 where the allowable diffuse derogation of 2.5 μA , 7.5 μA , and 10 μA for null reference, capture effect, and sideband reference has been used. As the figure indicates, the proposed cost of site grading is considerably less than current costs.

REFERENCES

1. J. L. Leader, "The Relationship Between the Kirchoff Approach and Small Perturbation Analysis in Rough Surface Scattering Theory," *IEEE Trans. on Antennas and Propagation*, AP-19, p. 786 (1971).
2. S. O. Rice, "Reflections of Electromagnetic Waves from Slightly Rough Surfaces," *Commun. Pure Appl. Math.*, vol. 4, p. 361 (1951).
3. A. K. Fung and H. L. Chan, "Back Scattering of Waves by Composite Rough Surfaces," *IEEE Trans. on Antennas and Propagation*, AP-17, p. 590 (1969).
4. M. L. Burrows, "On the Composite Model for Rough-Surface Scattering," *IEEE Trans. on Antennas and Propagations*, AP-21, p. 241 (1973).
5. G. R. Valenzuela, "Scattering of Electromagnetic Waves by a Tilted Slightly Rough Surface," *Radio Science*, vol. 3, p. 1057 (1968).
6. P. Beckmann, "Scattering by Composite Rough Surfaces," *Proc. of the IEEE*, vol.53, p. 1012 (1965).
7. H. G. Weiss, "Air Traffic Control," *Quarterly Summary*, Lincoln Laboratory, Mass. Institute of Technology, Lexington, Mass., p. 3 (1972).
8. T. B. A. Senior, "The Diffraction of a Dipole Field by a Perfectly Conducting Half-Plane," *Quant. Journal Mech. and Applied Math.*, vol. VI, pt. 1, p. 101 (1953).
9. B. D. Woods, "The Diffraction of a Dipole Field by a Half-Plane," *Quant. Journal Mech. and Applied Math.*, vol. X, pt. 1, p. 90 (1957).
10. T. J. I'A. Bromwich, *Proc. London Math Soc.*, 14, pg. 450 (1915).

11. M. Born and E. Wolf, Principles of Optics, Pergamon Press, New York, p. 565 (1959).
12. J. T. Godfrey, H. F. Hartley, G. J. Moussally, and R. A. Moore, "Terrain Modeling Using the Half-Plane Geometry with Applications to ILS Glide Slope Antennas," to be published in IEEE Trans. on Antennas and Propagation.
13. P. Beckmann and A. Spizzichino, The Scattering of Electromagnetic Waves from Rough Surfaces, The MacMillan Co., New York, p. 220 (1963).
14. G. F. Jiracek, "Numerical Comparison of a Modified Rayleigh Approach with Other Rough Surface EM Scattering Solutions," IEEE Trans. on Antennas and Propagation, AP-21, no. 3, p. 393 (1973).
15. Siting Criteria for Instrument Landing Systems, Department of Transportation, no. 6750.16A, DOT, FAA, Washington, D. C., p. 46 (1973).
16. J. E. Freund, Mathematical Statistics, Prentice-Hall, Inc., Englewood Cliffs, N. J., p. 373 (1971).
17. D. E. Barrick, "Rough Surface Scattering Based on the Specular Point Theory," IEEE Trans. on Antennas and Propagation, AP-16, no. 4, p. 449 (1968).
18. J. G. Lucas, private communication, Air Navigation Group, University of Sidney, Sidney, Australia (1975).

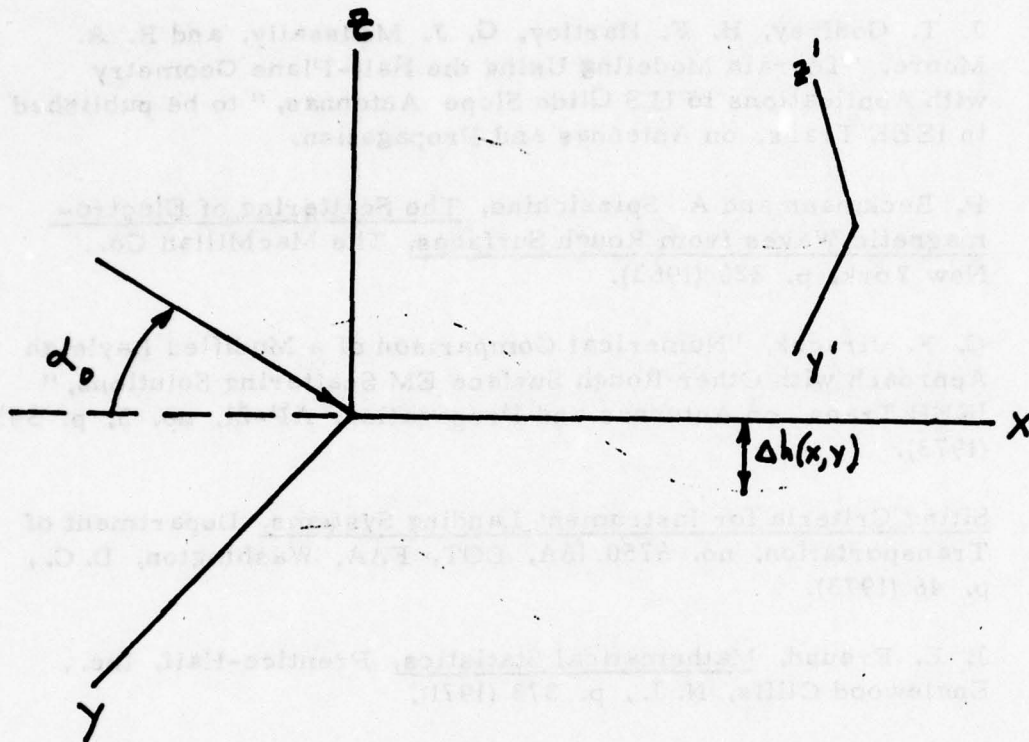


Figure II-1. Definition of Coordinate Systems Illustrating Space and Local Coordinate Geometries

Fig. II 3a.

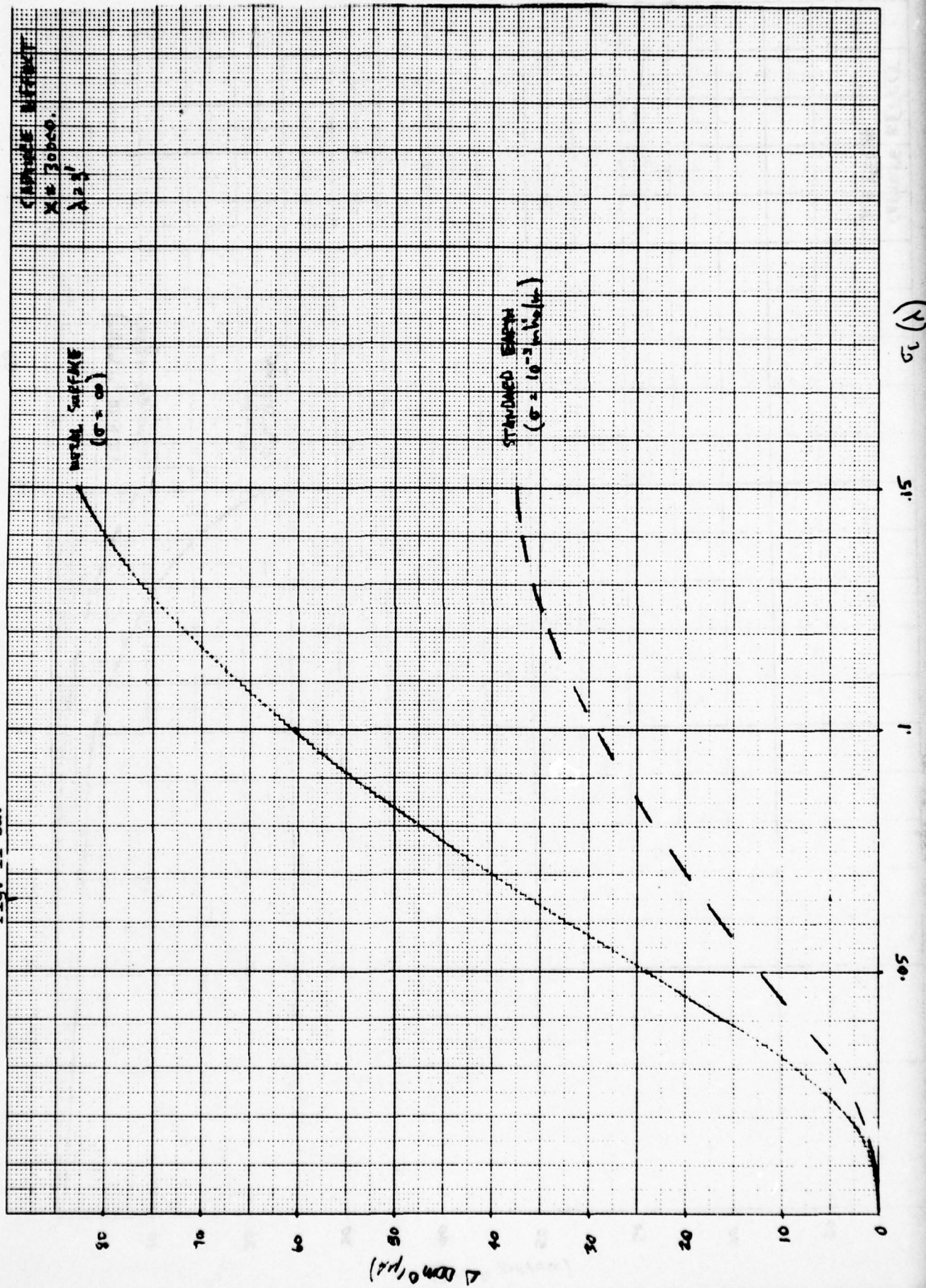


Fig. II 3b

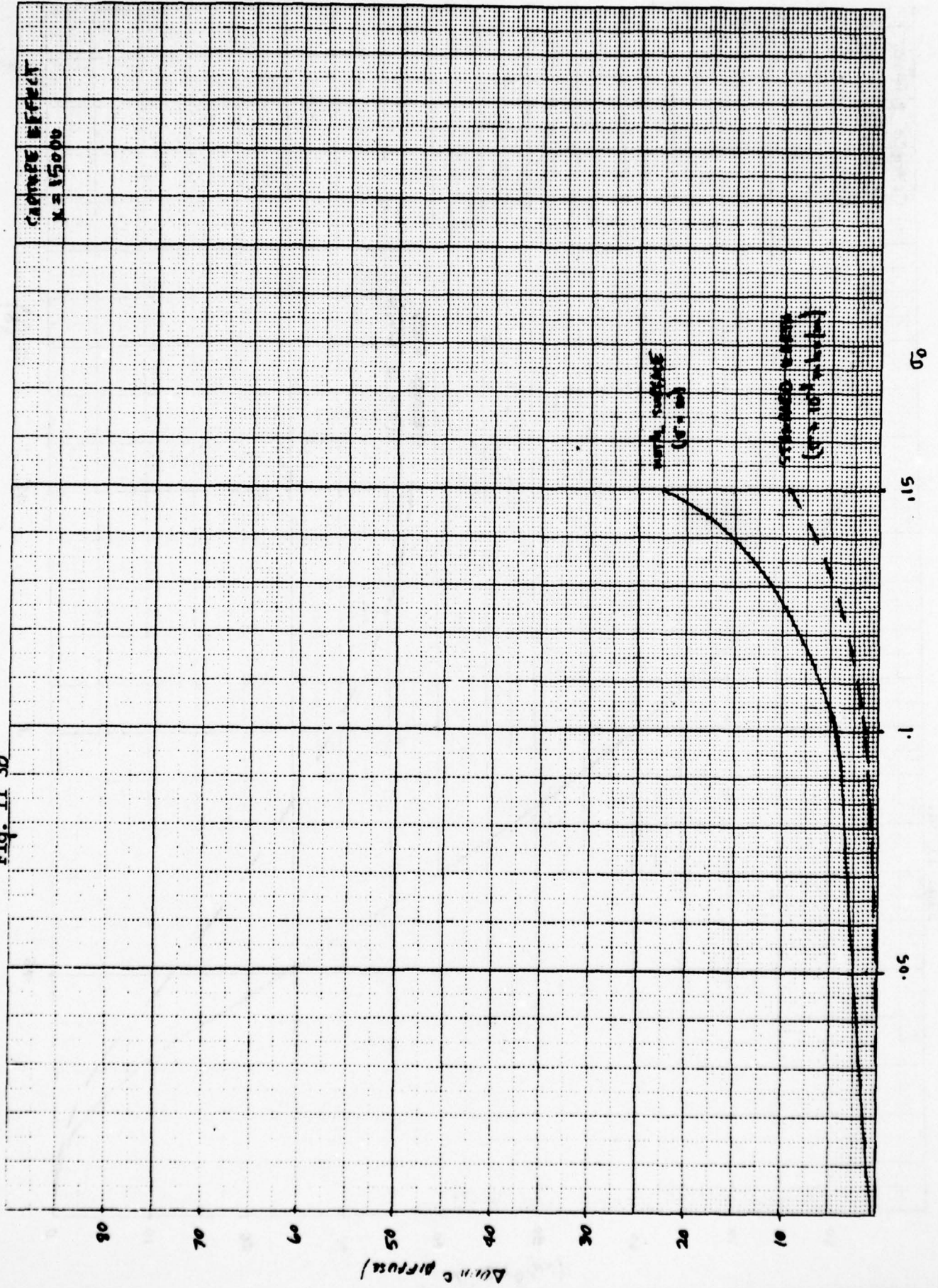


Fig. II 3c

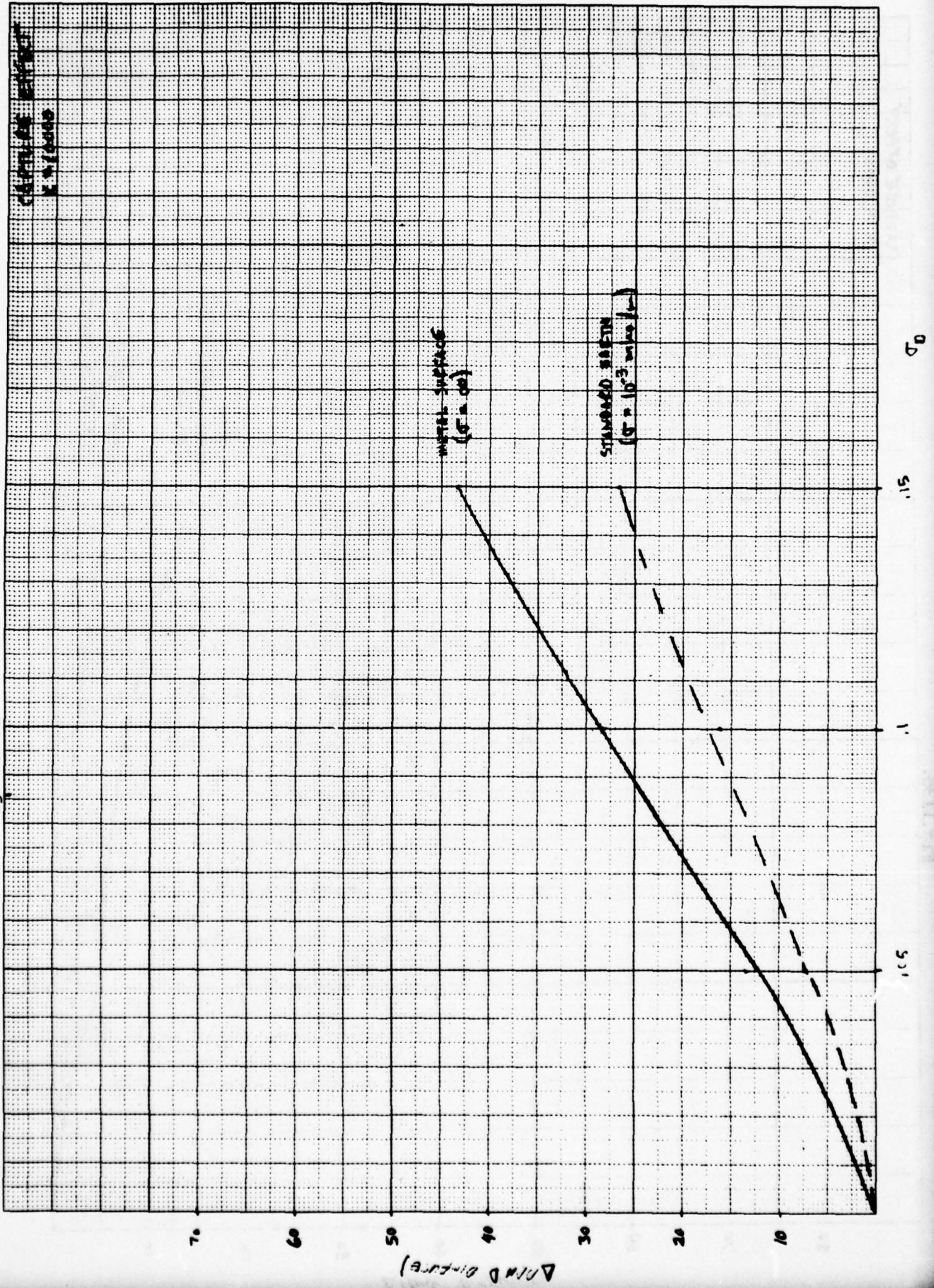


Fig. II3d.

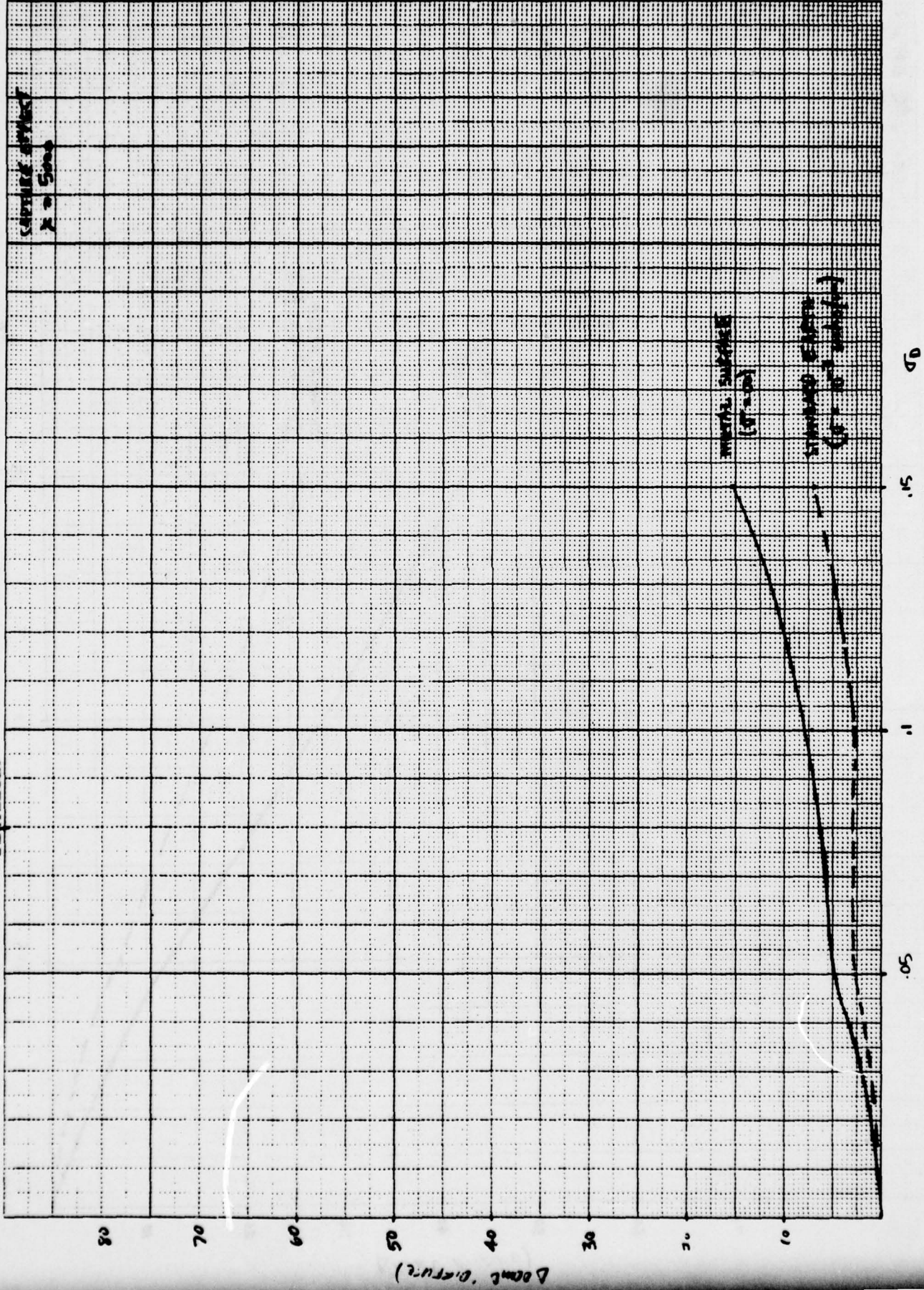


Fig. II3e.

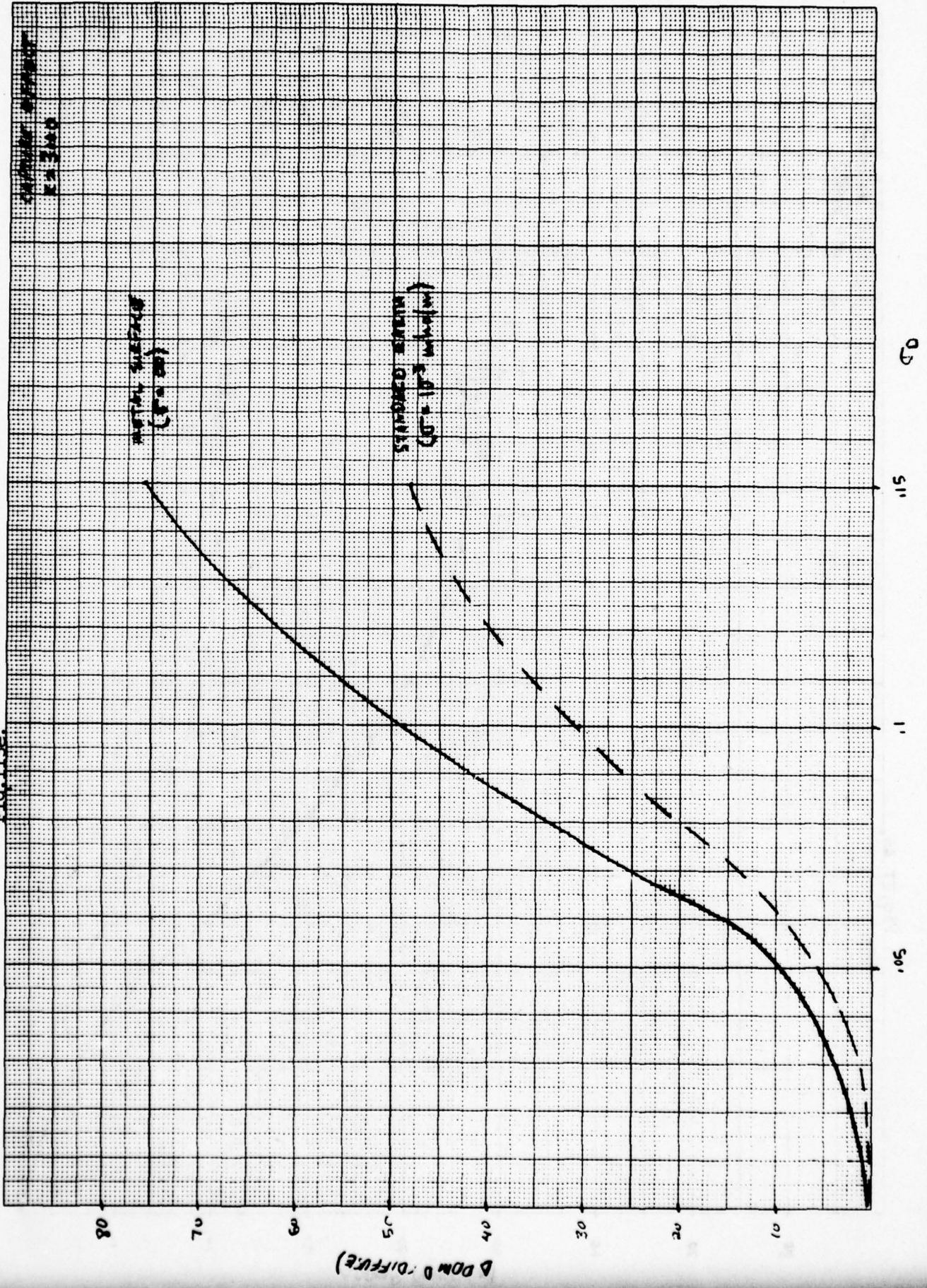


Fig. II 4a

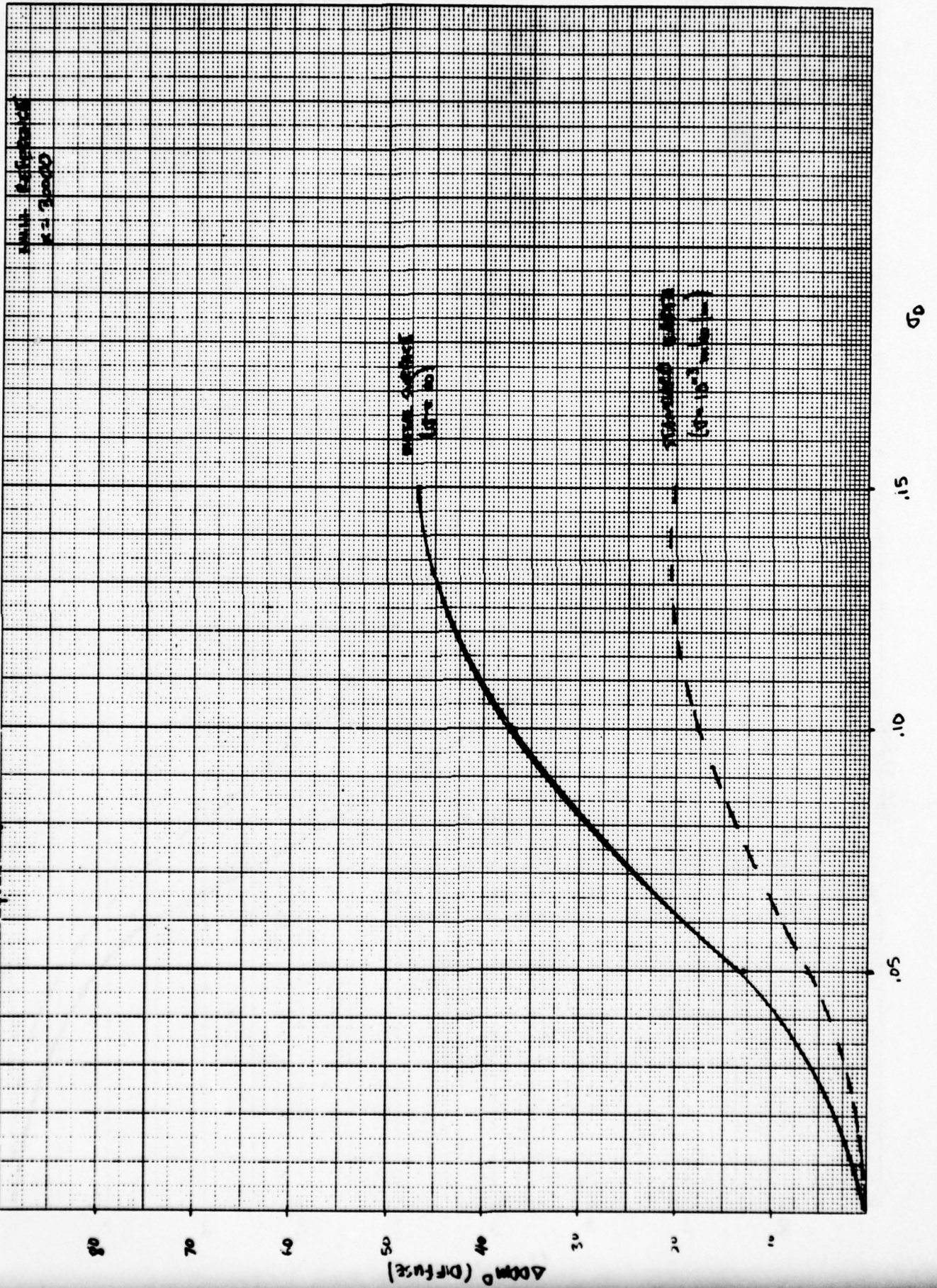


Fig. II 4b

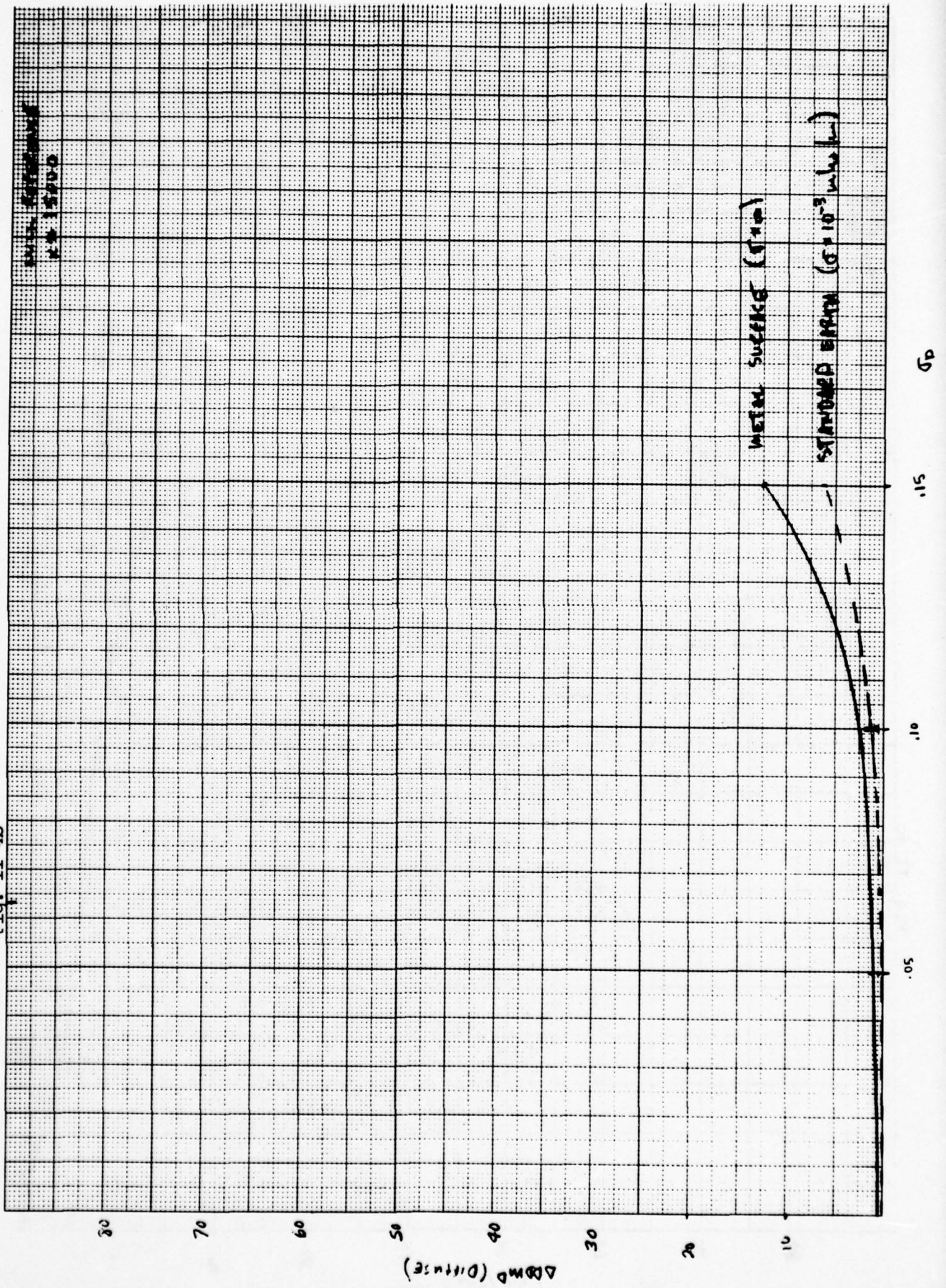


Fig. II 4c

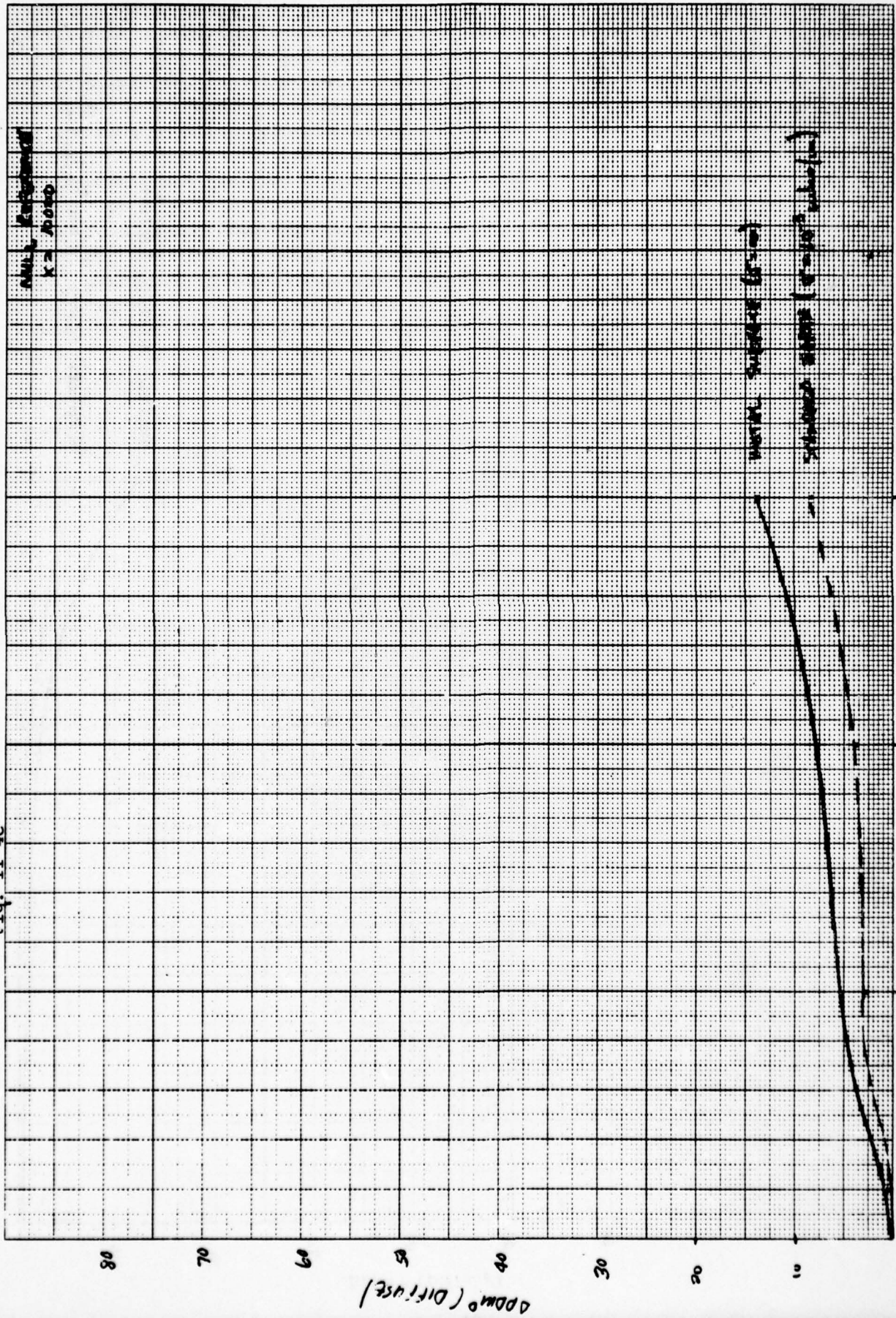


Fig. II 4d

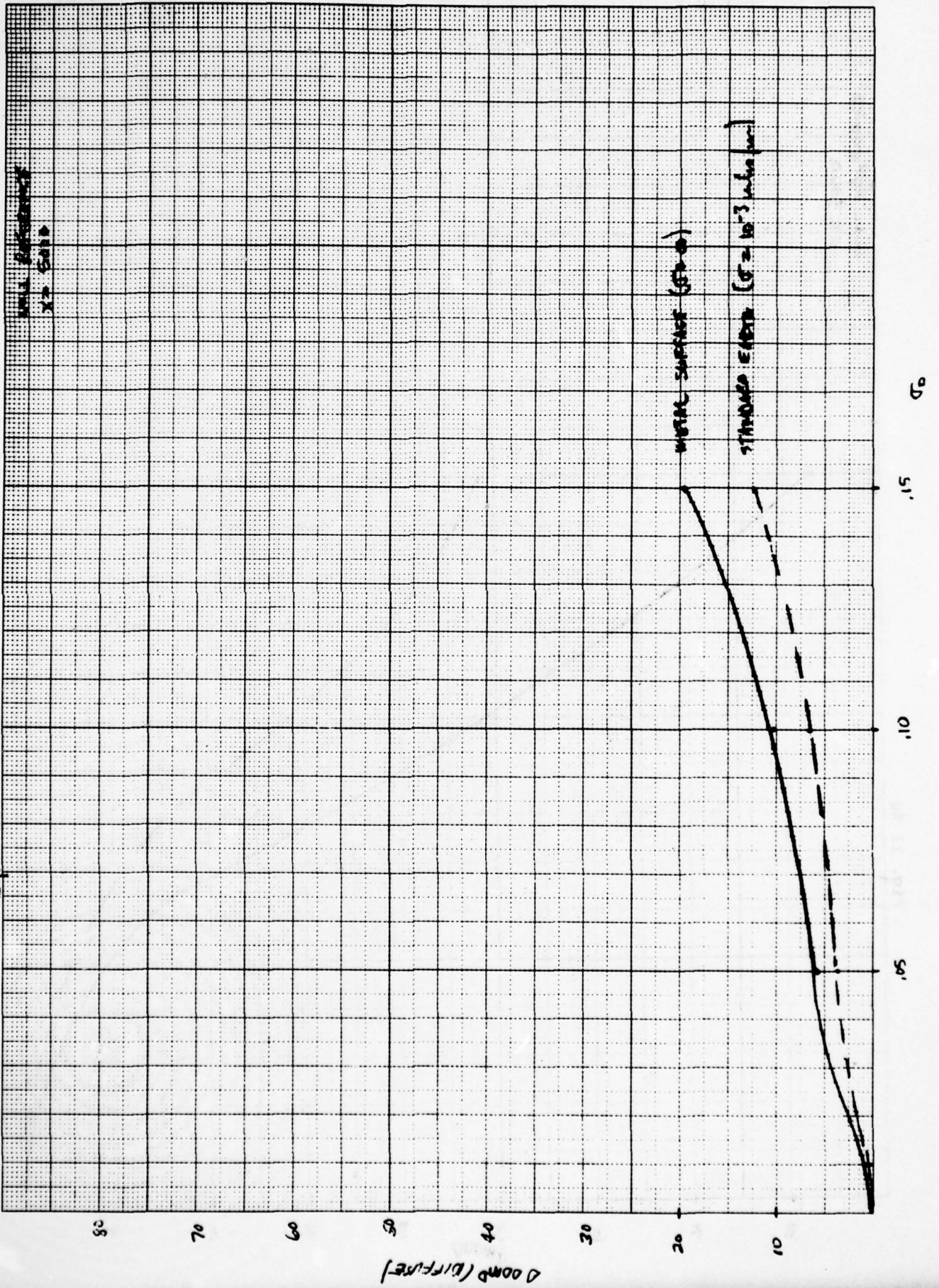


Fig. II 4e

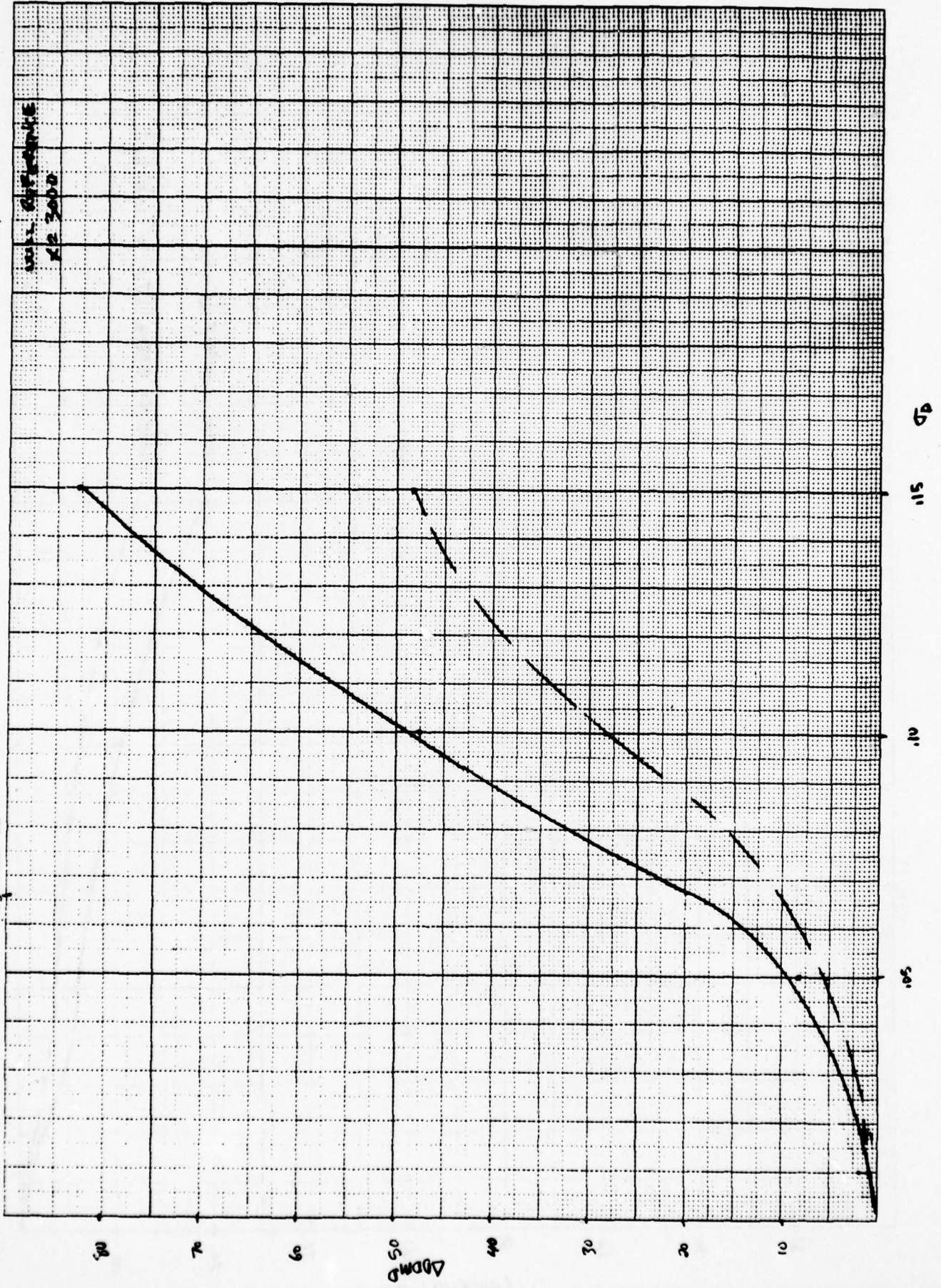


Fig. II 5a

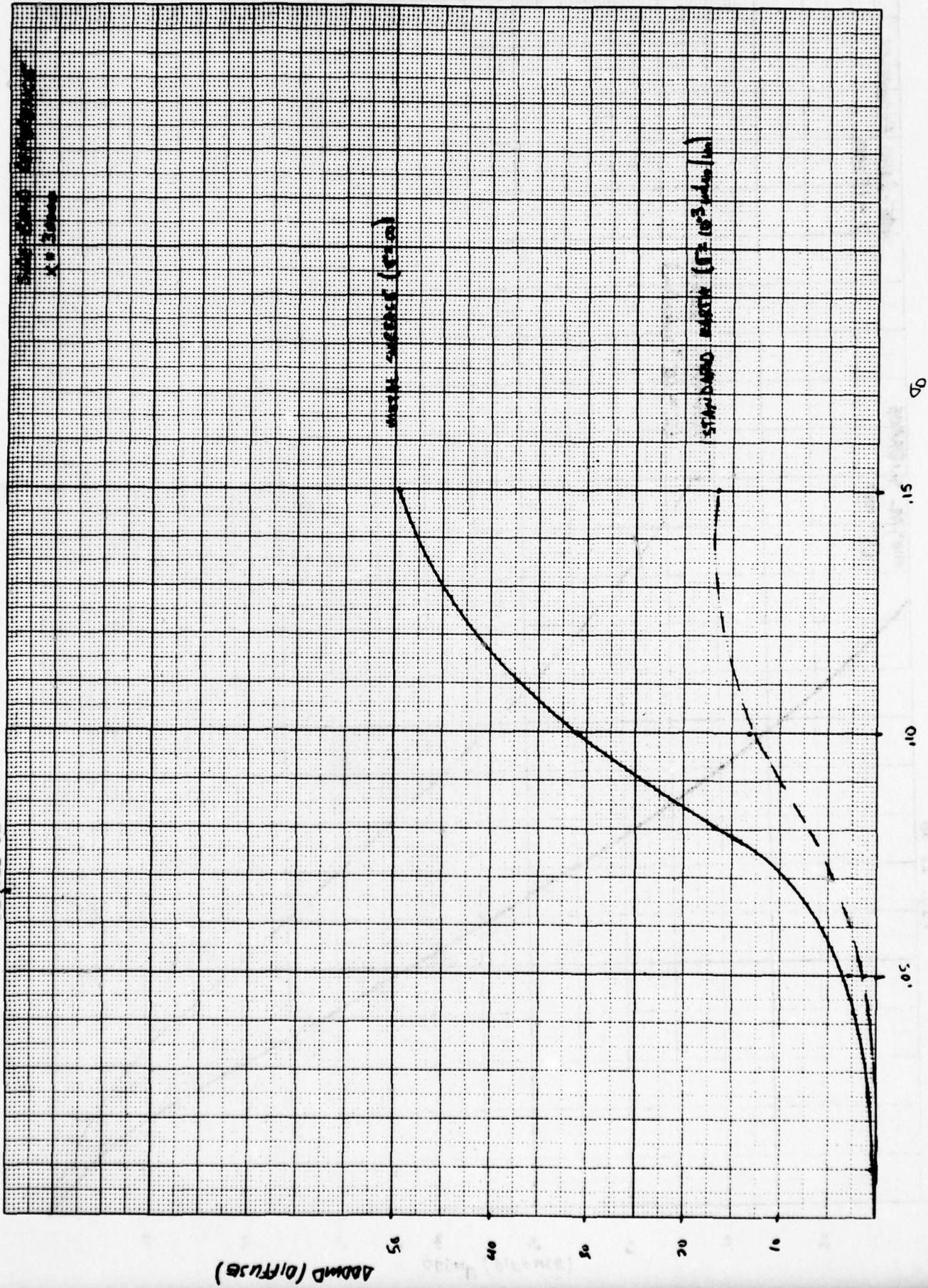
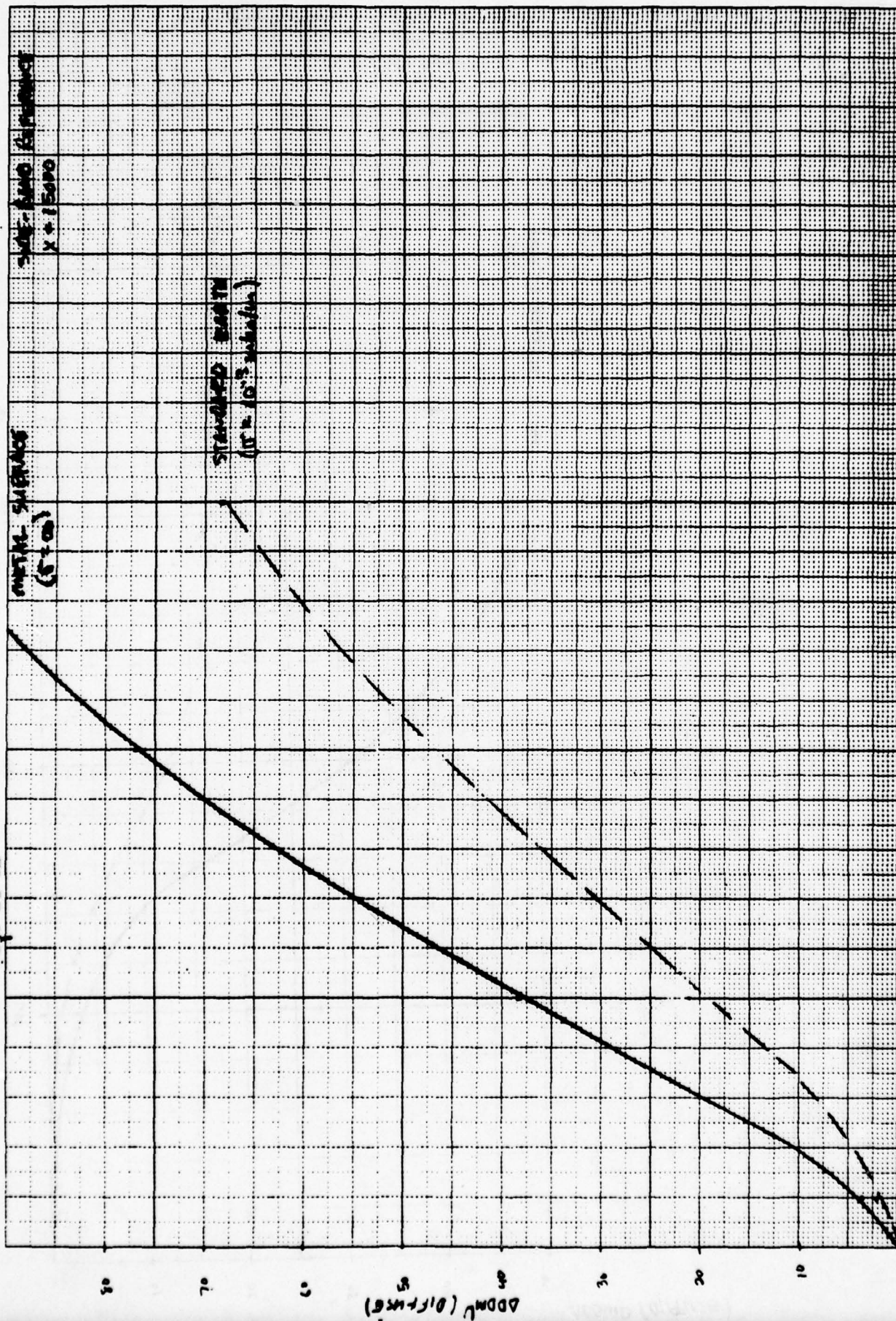


Fig. II 5b

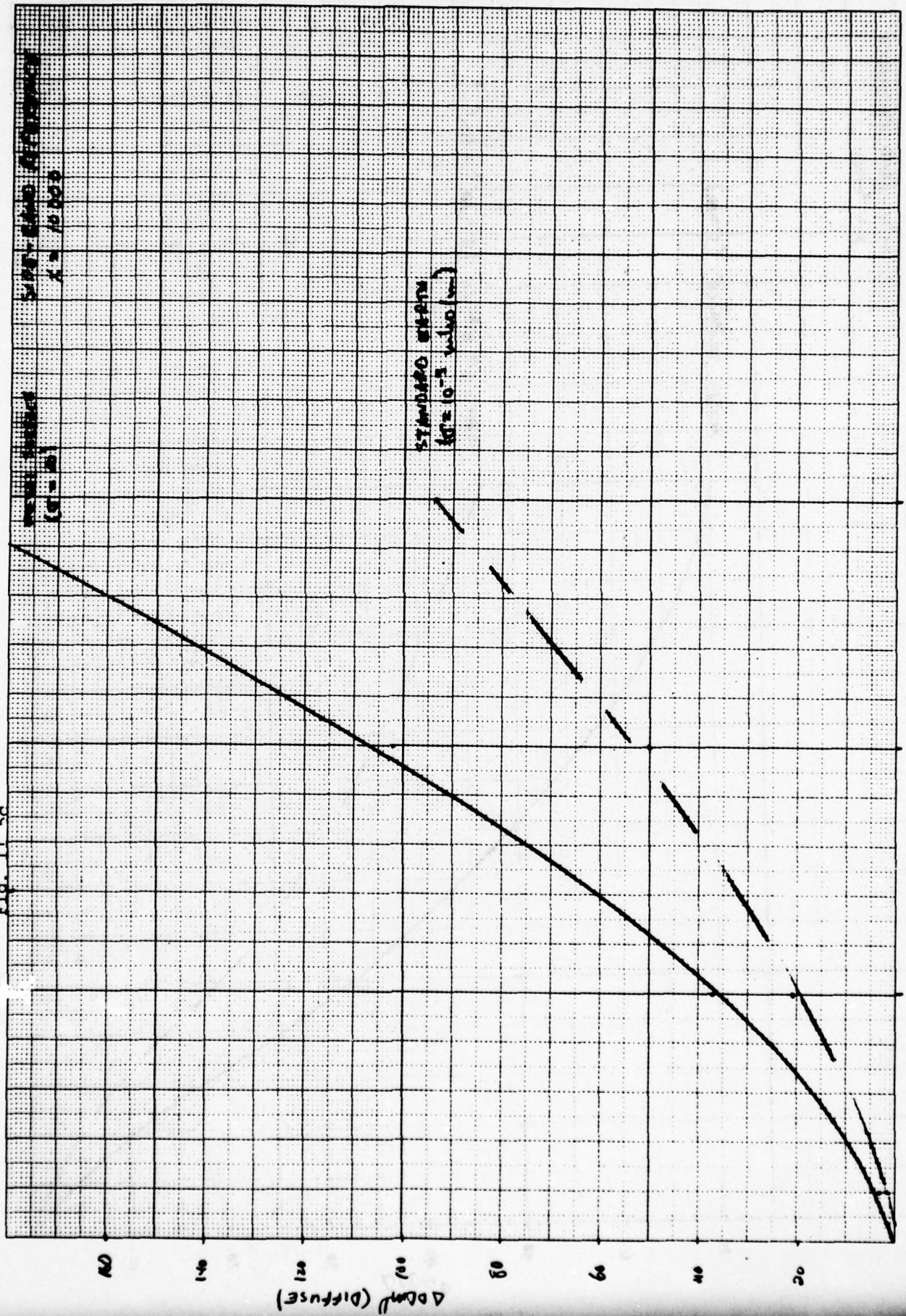


ADDMV (DIFFERS)
X = 15000

STANDARD SENSORS
(10% 10'S SENSORS)

0.05 0.10 0.15 0.20

Fig. II 5c



59 10 15 50

Fig II 5D

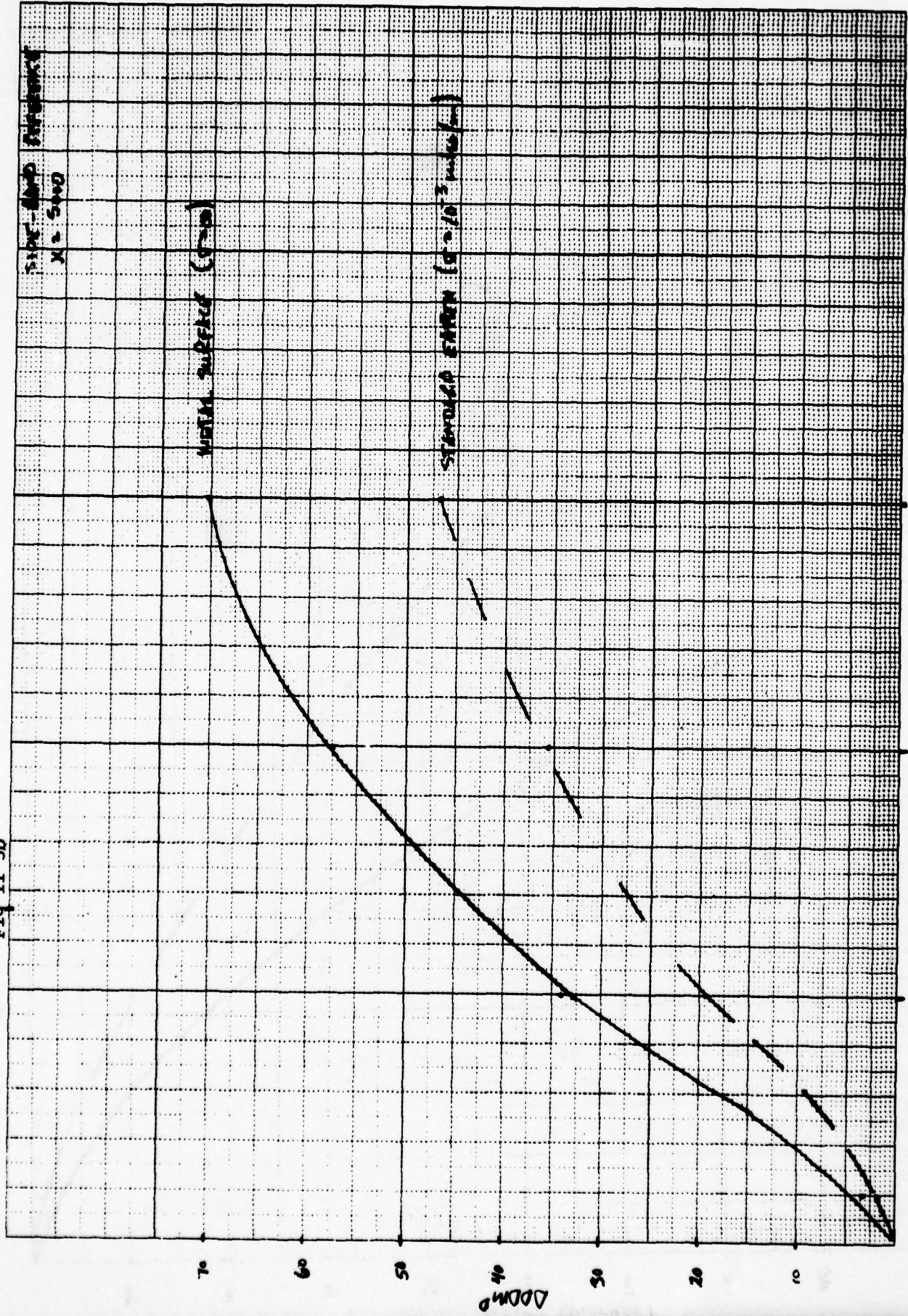
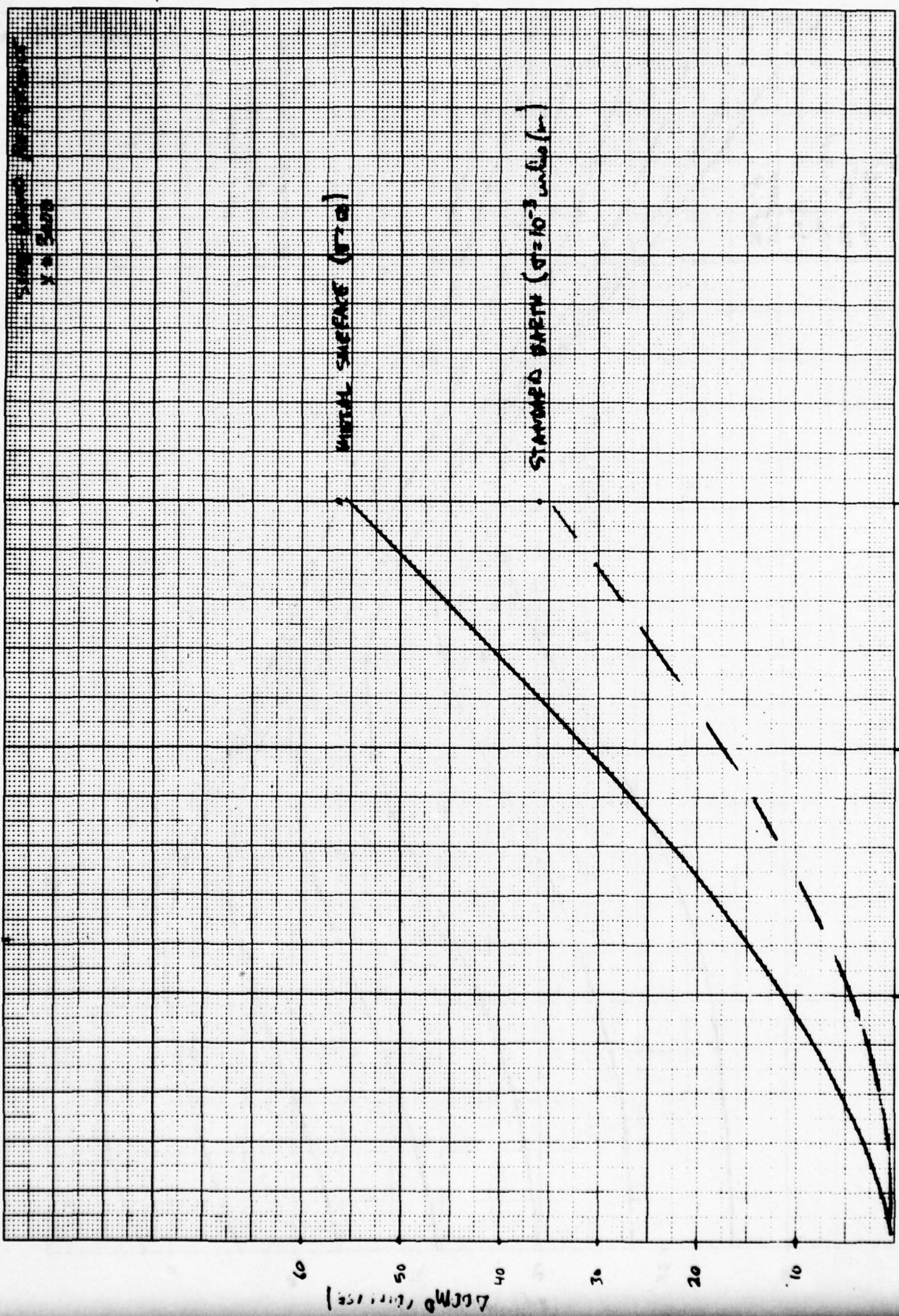


Fig II 5e.



Y. S. SUN

INITIAL SURFACE (WTO)

STAMPED SURFACE (σ = 10³ units/in²)

LUMEN TRANSMITTANCE

.05 .10 .15 .20

Fig. II 6a

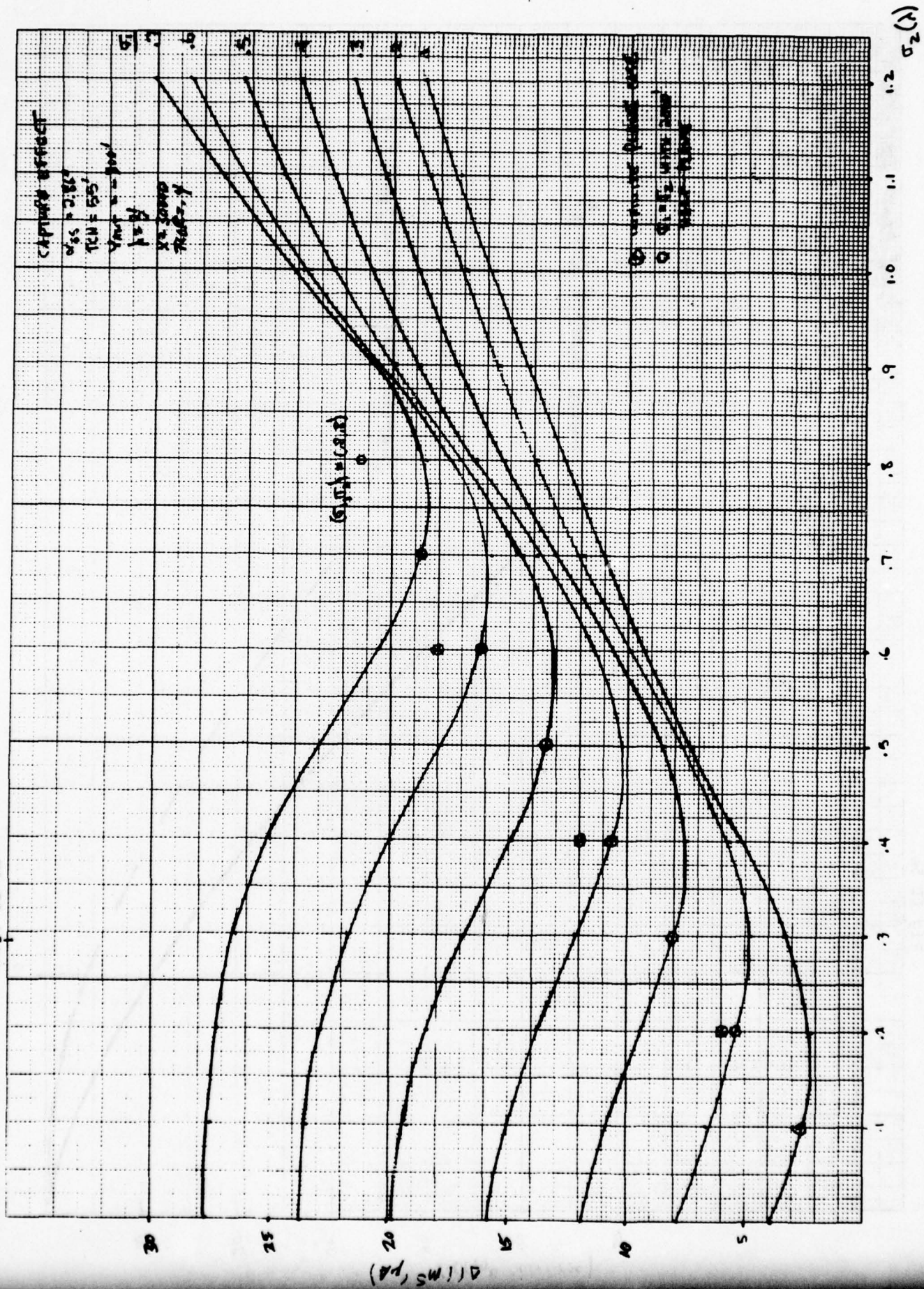


Fig. II 6b

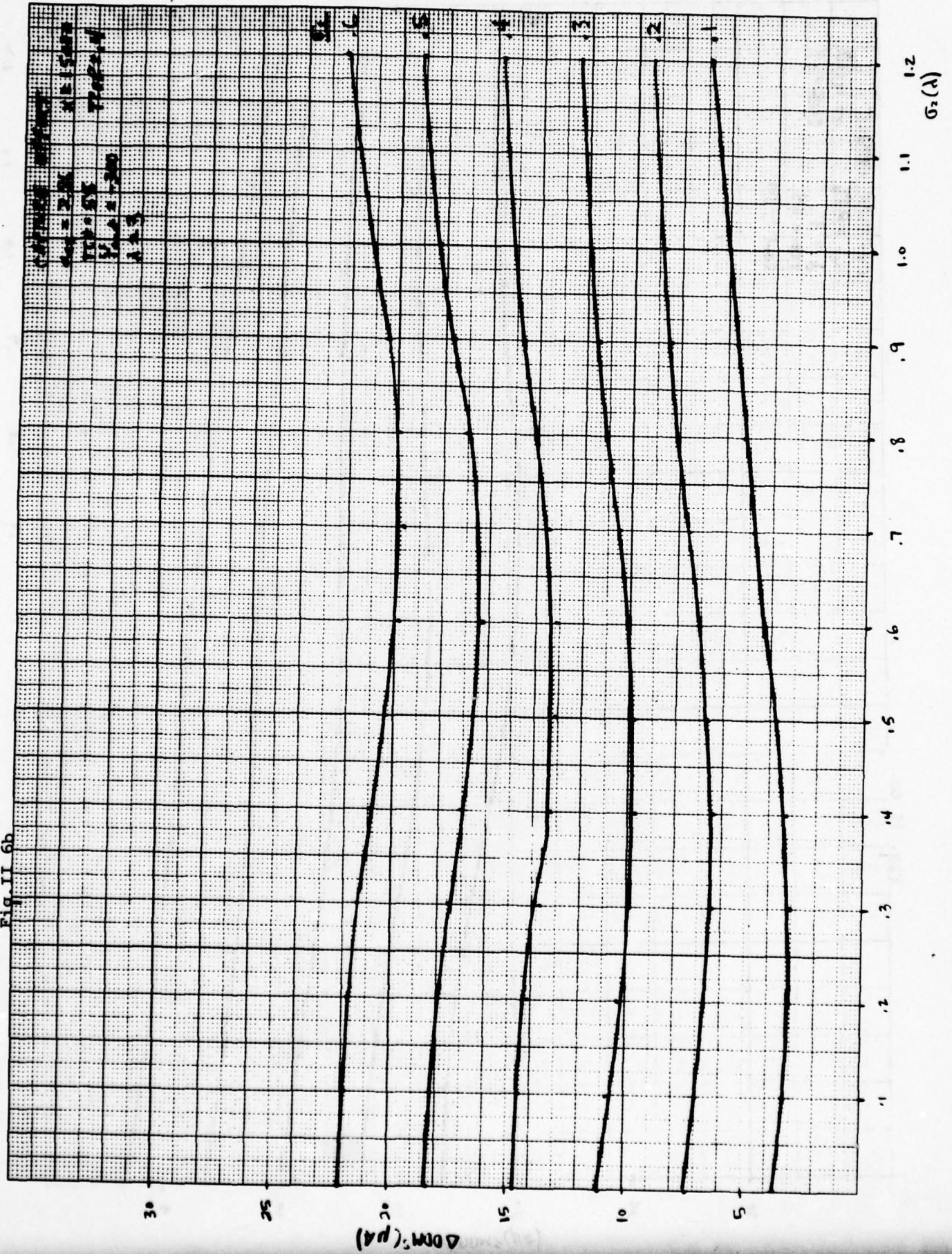


Fig. II 6c.

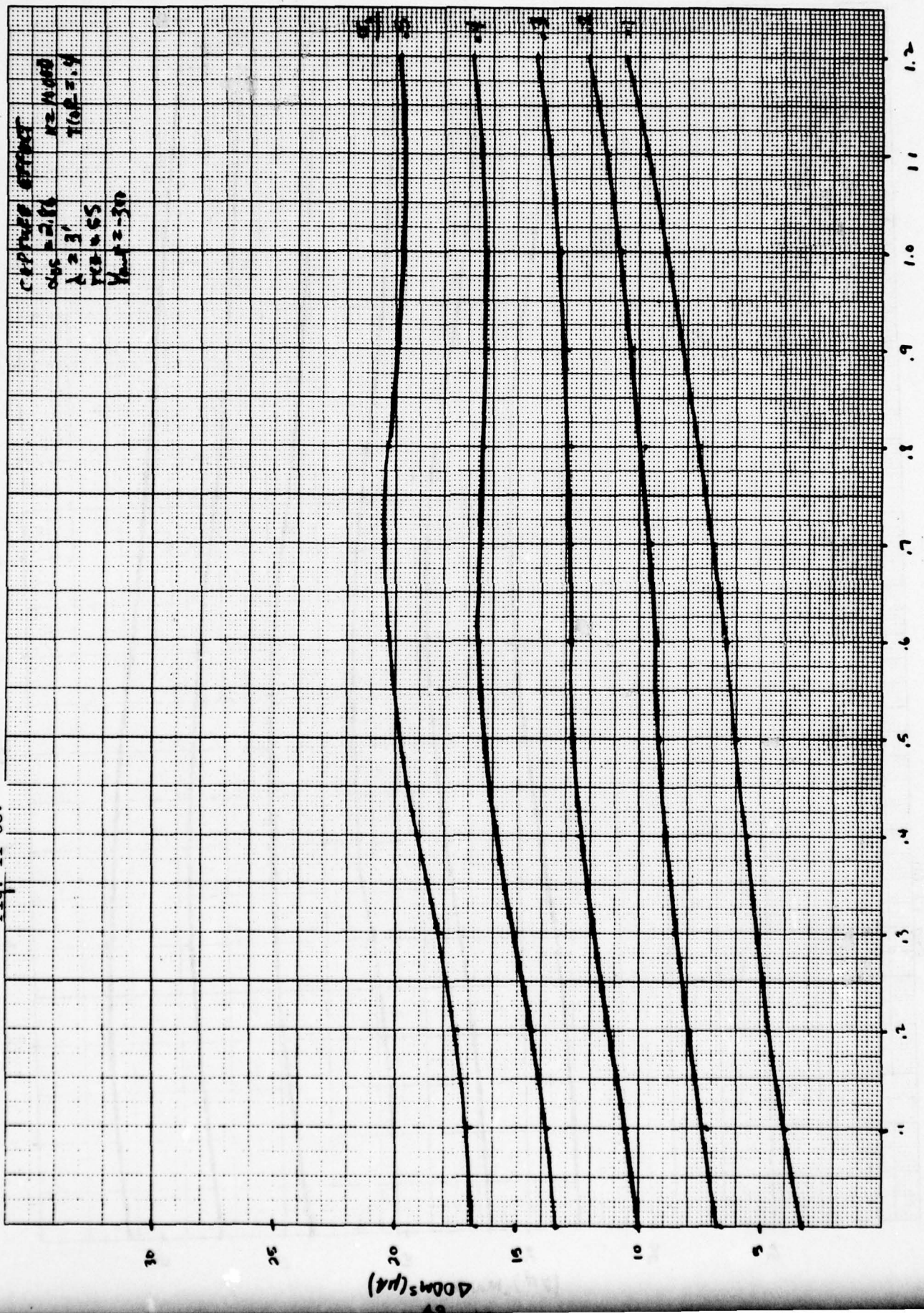


Fig. II 6d

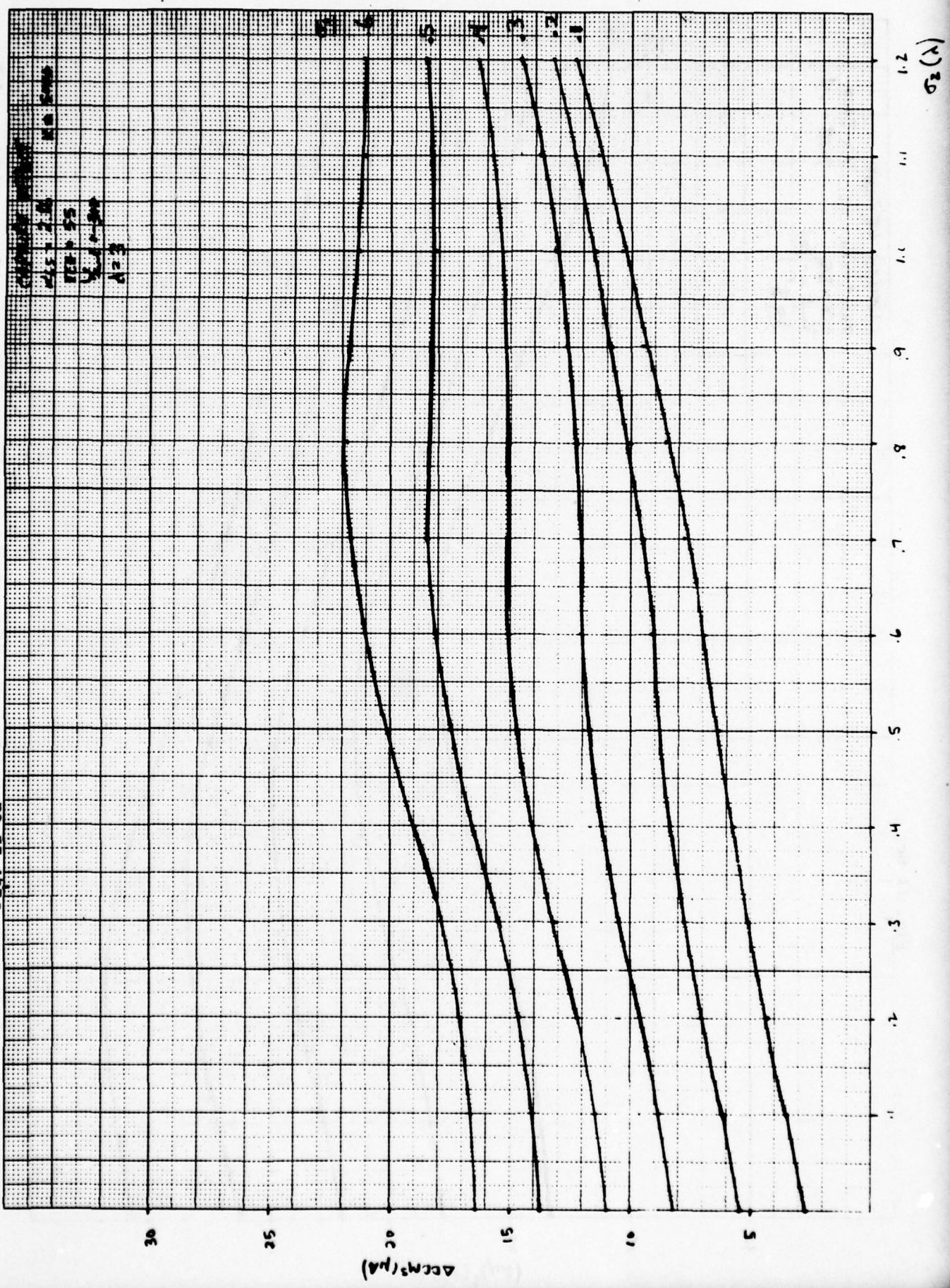


Fig. II 6e.

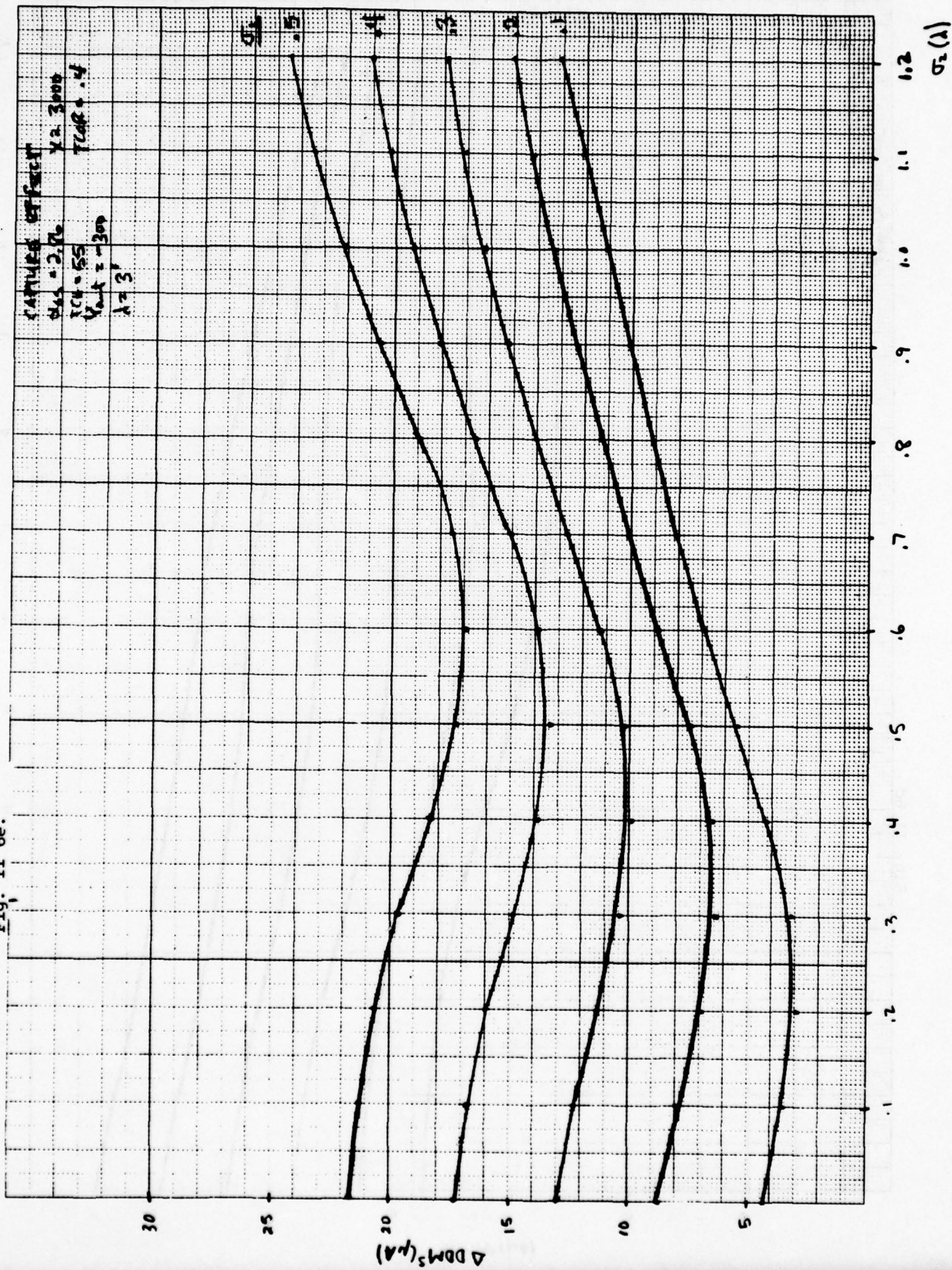


Fig. II 7a

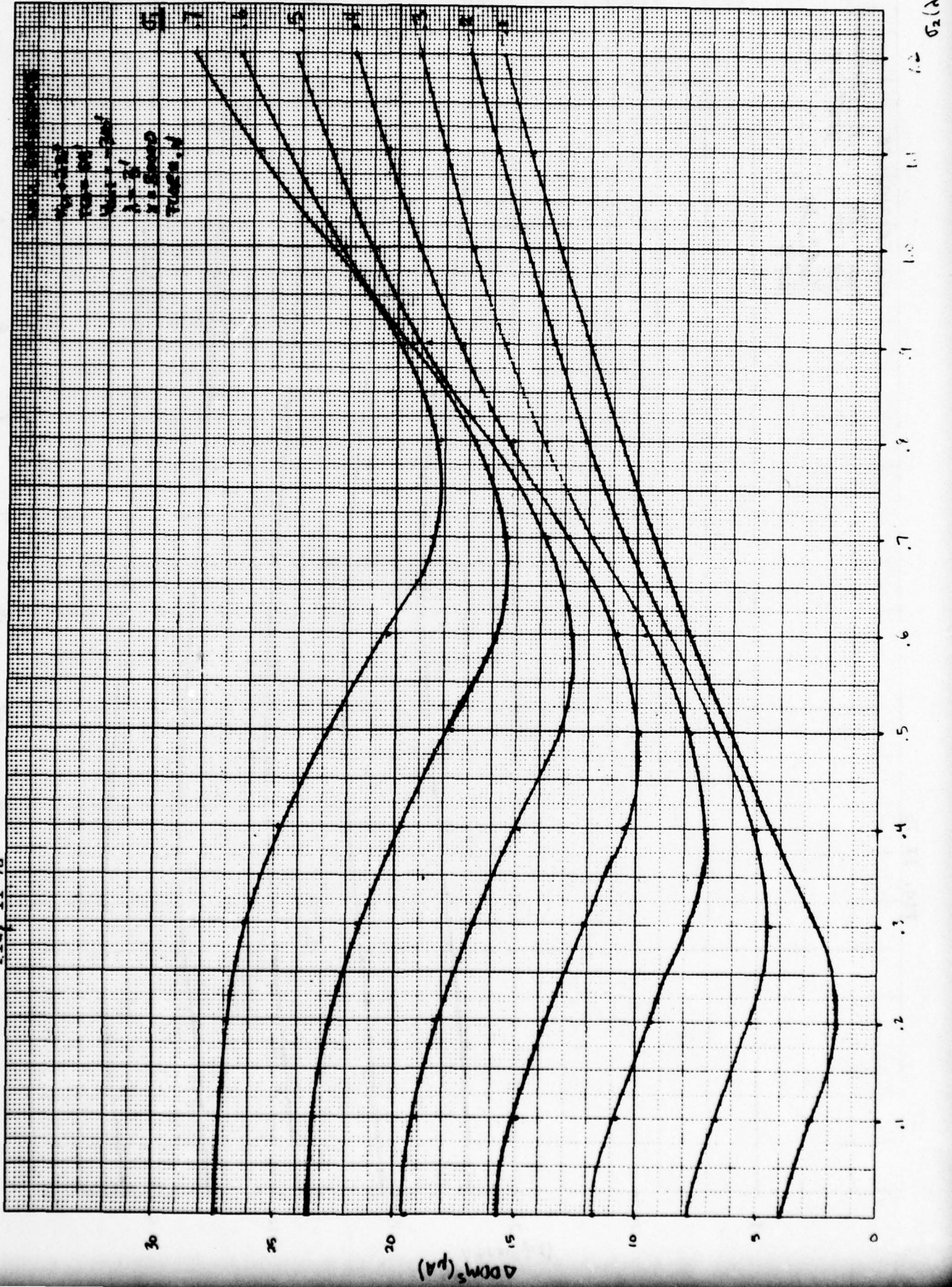


Fig. II 7b

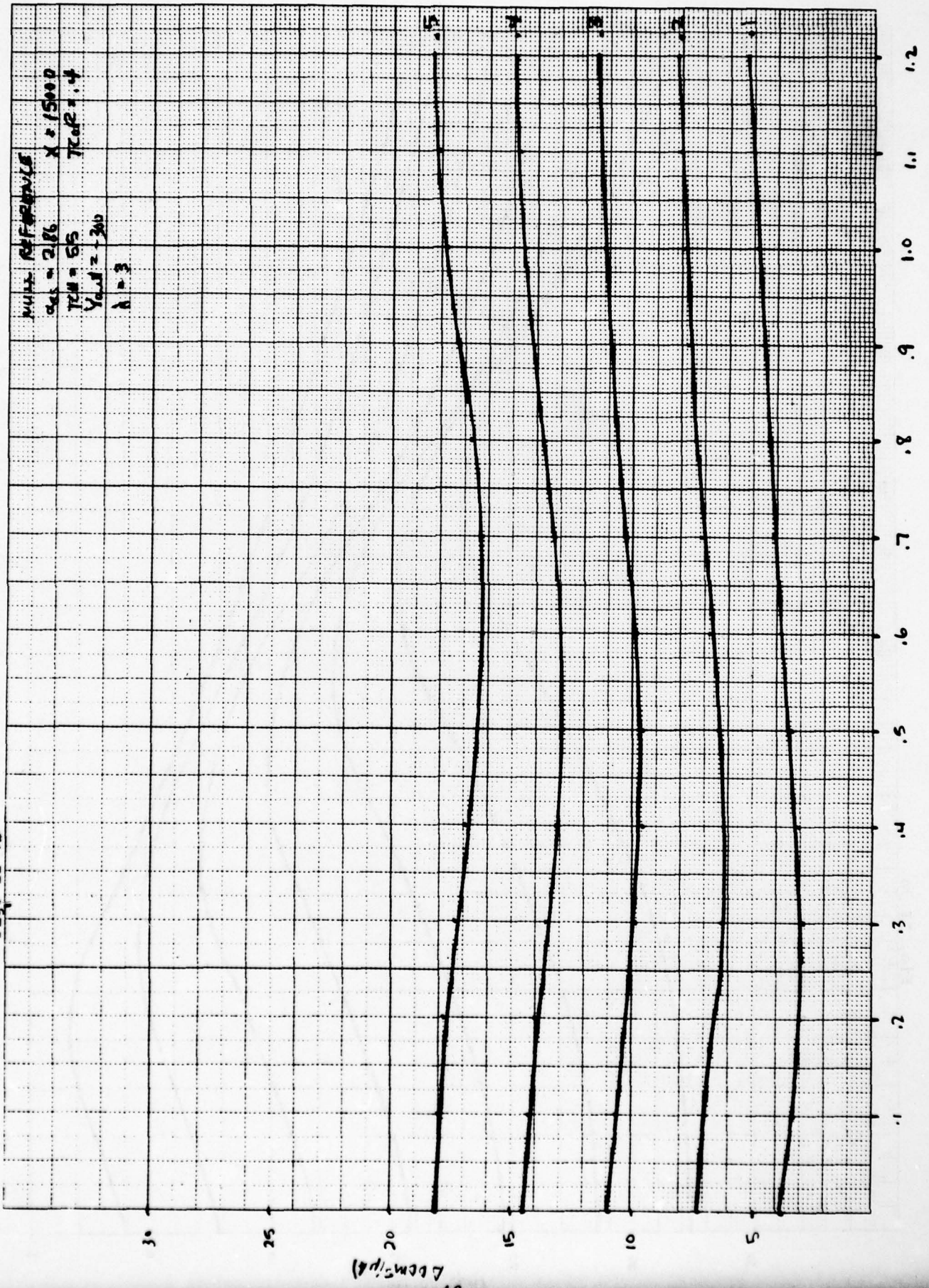


FIG. II.7C

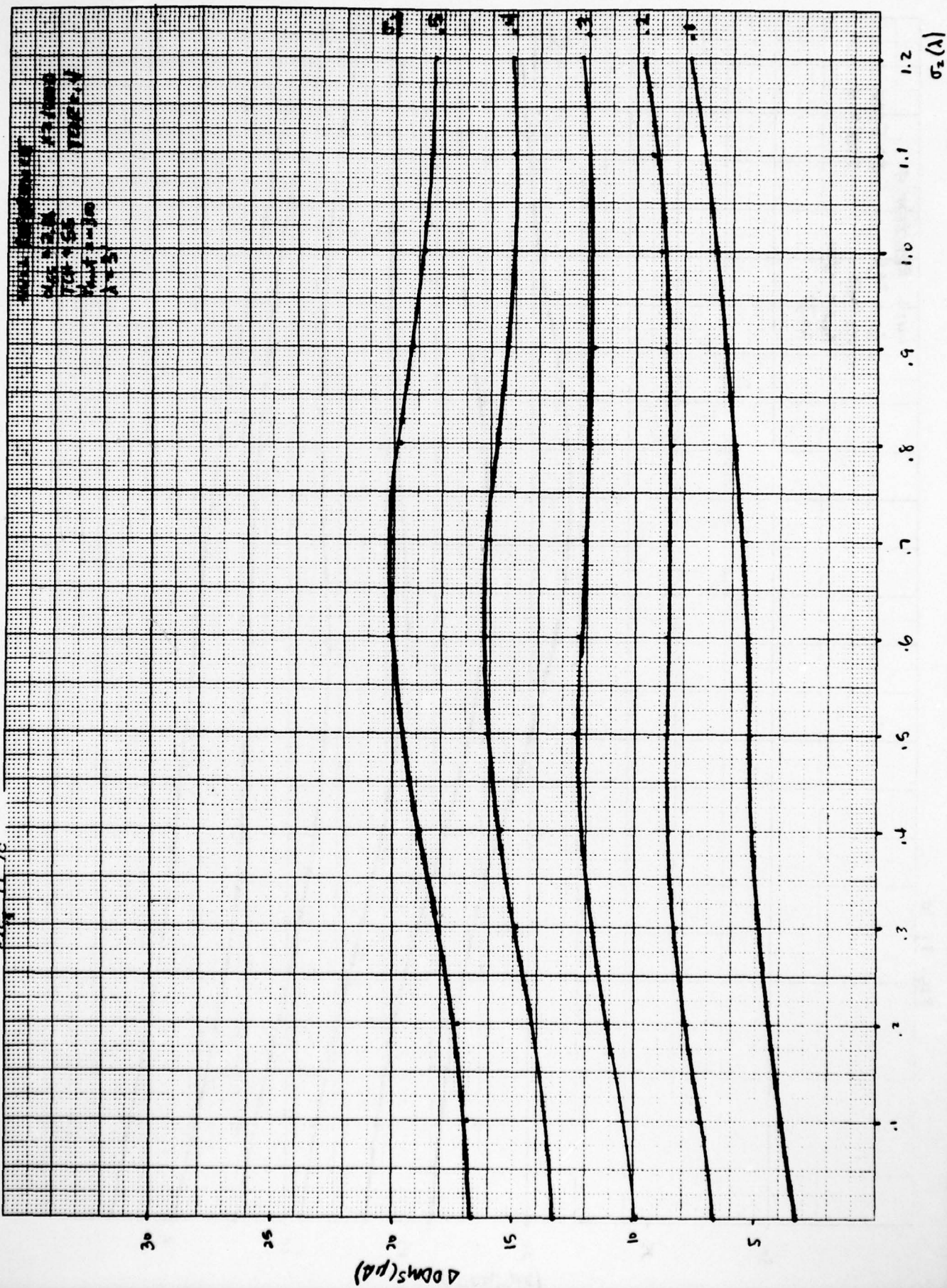


Fig. II 7d

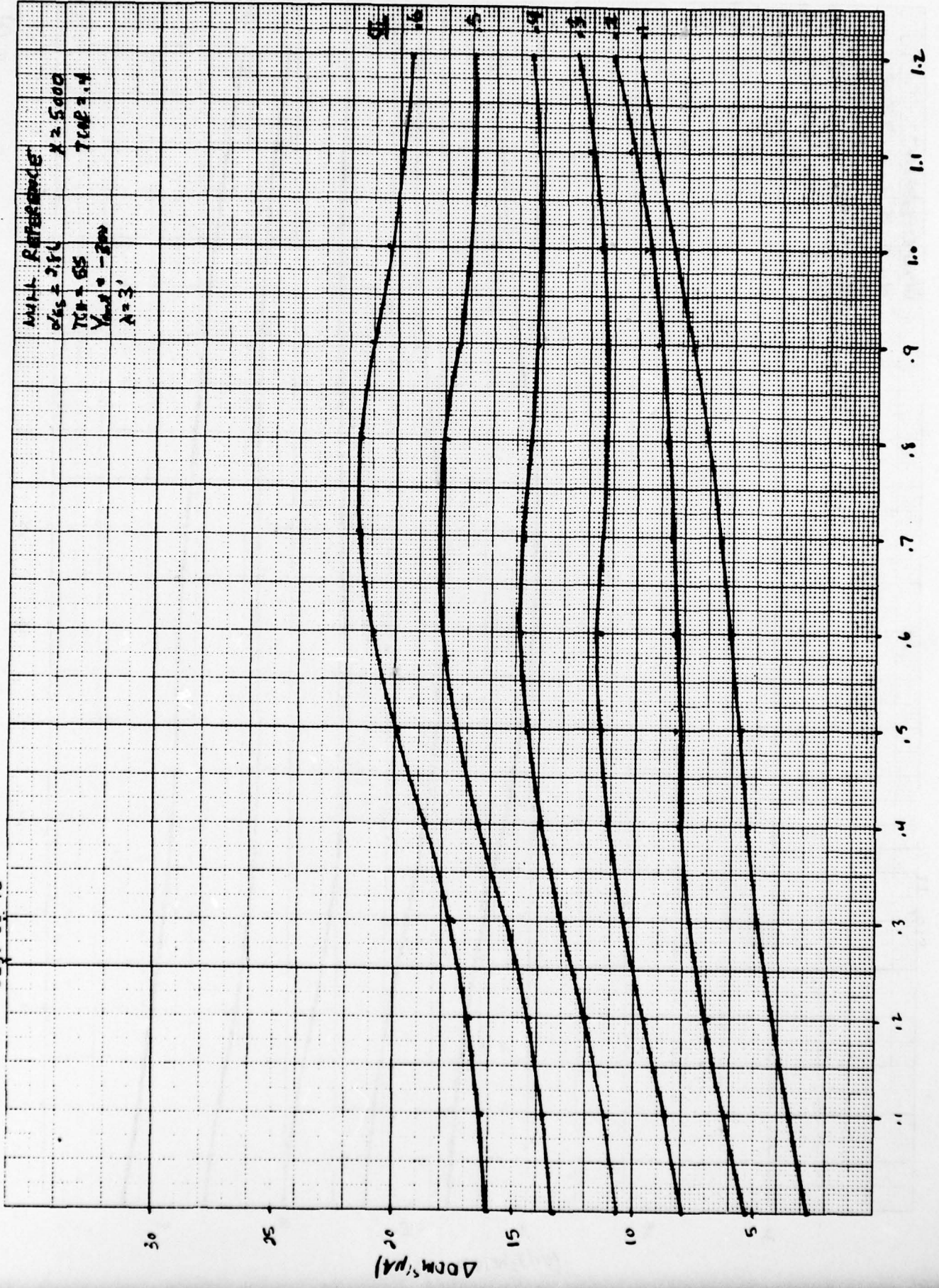


Fig. II 7e.

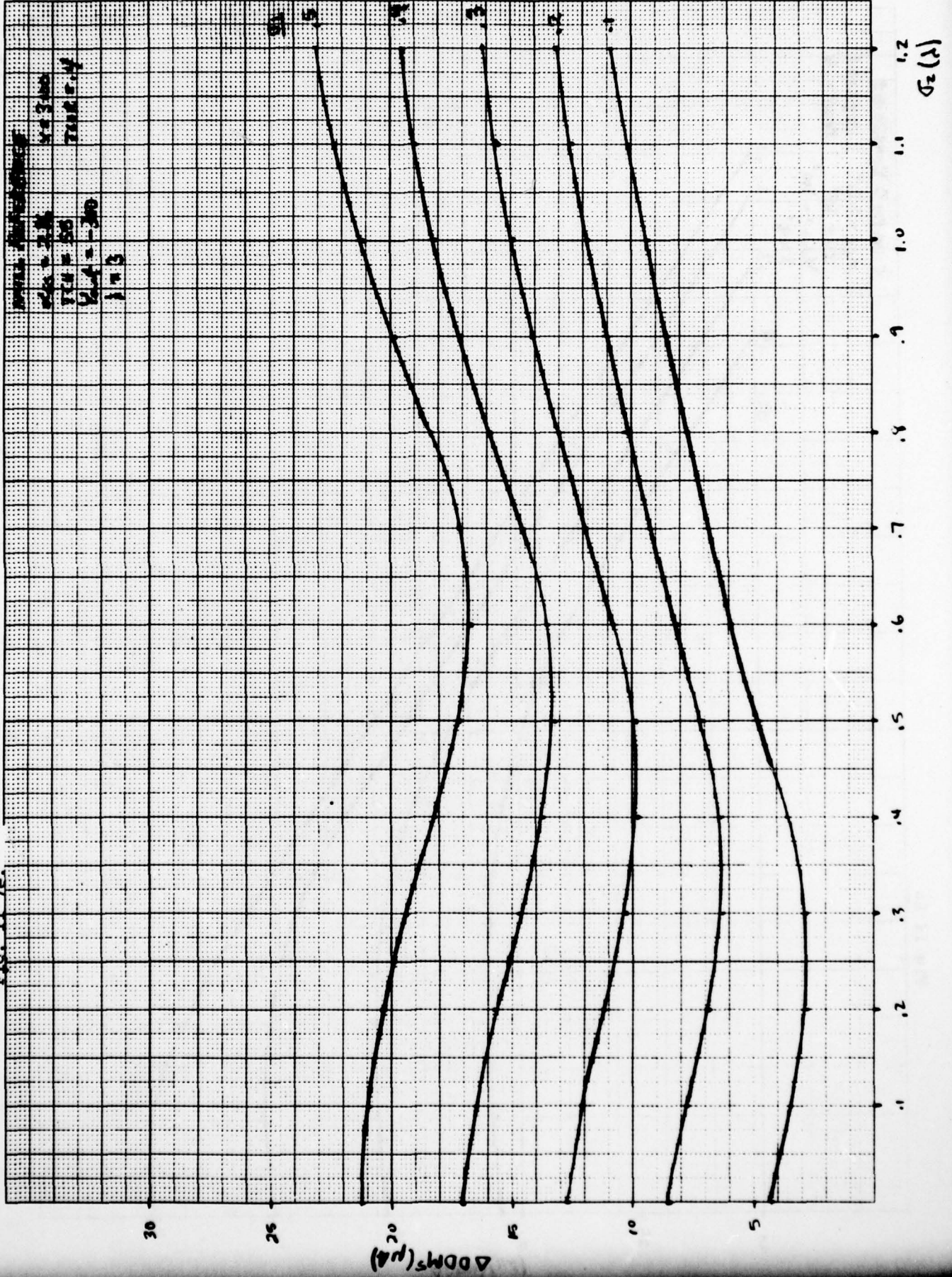


Fig II Ee

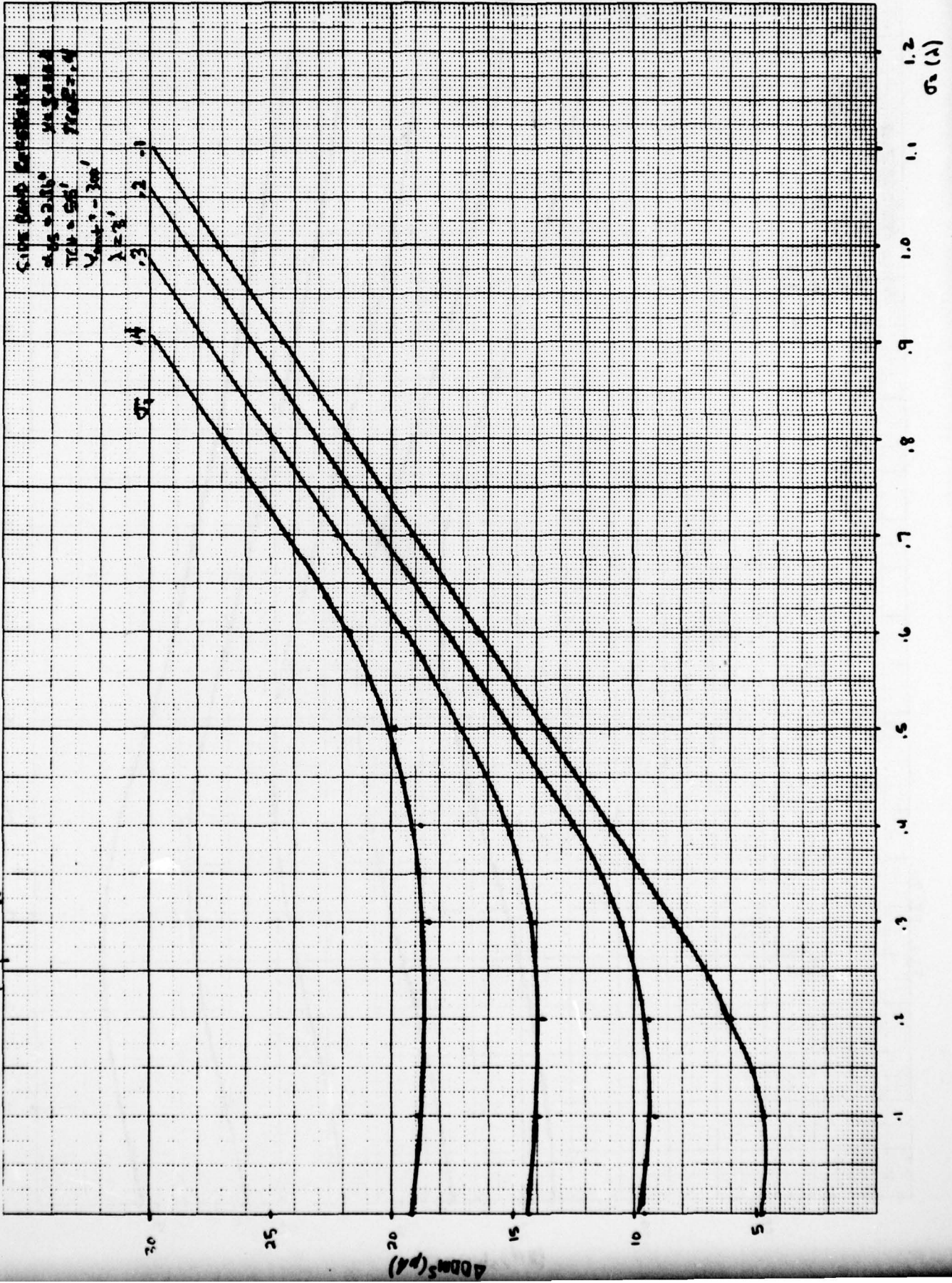
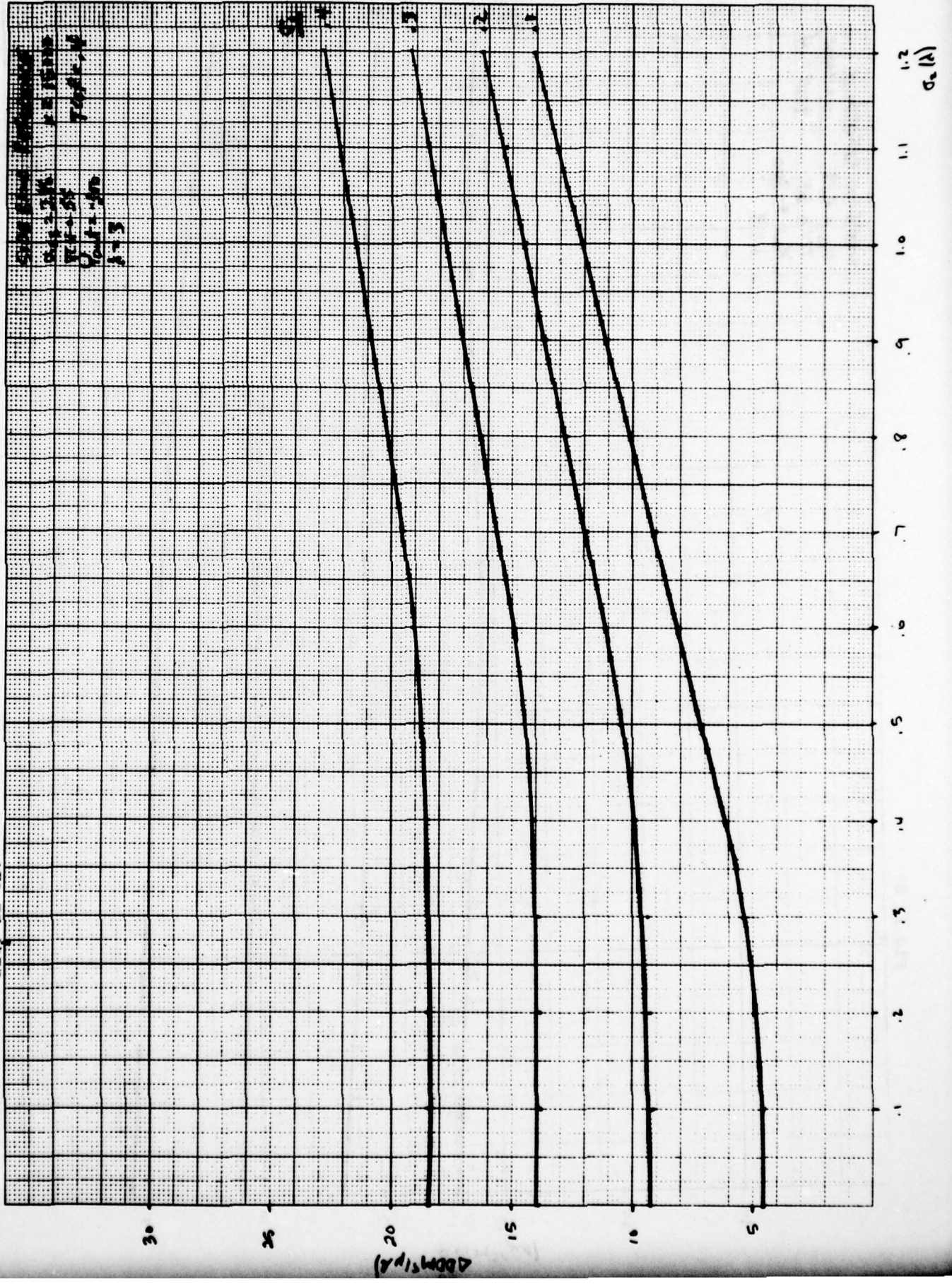


Fig. II 8b.



СЕРИЯ
№ 1-3
№ 1-3
№ 1-3

Fig. II 8c

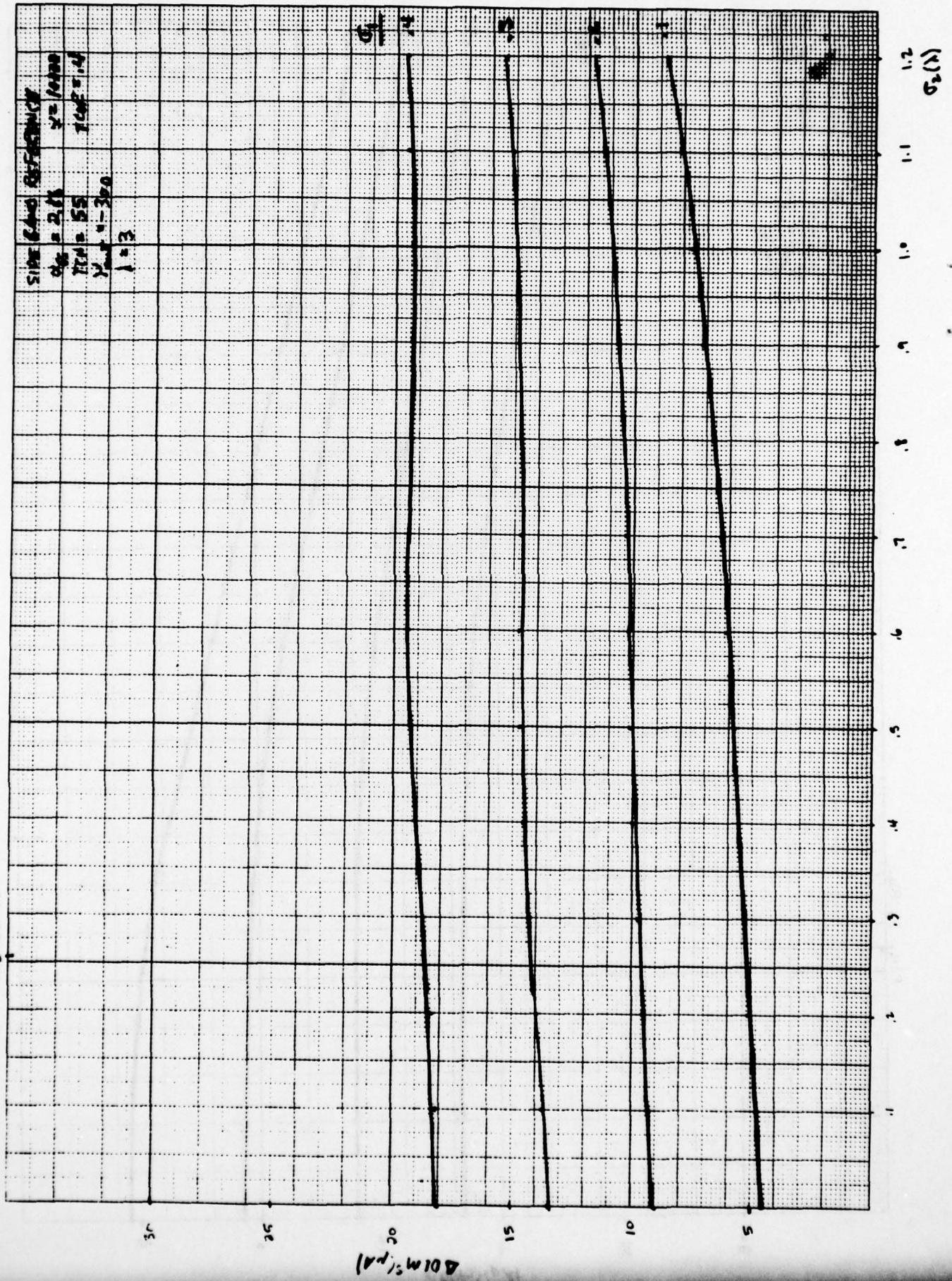


Fig II. 8d.

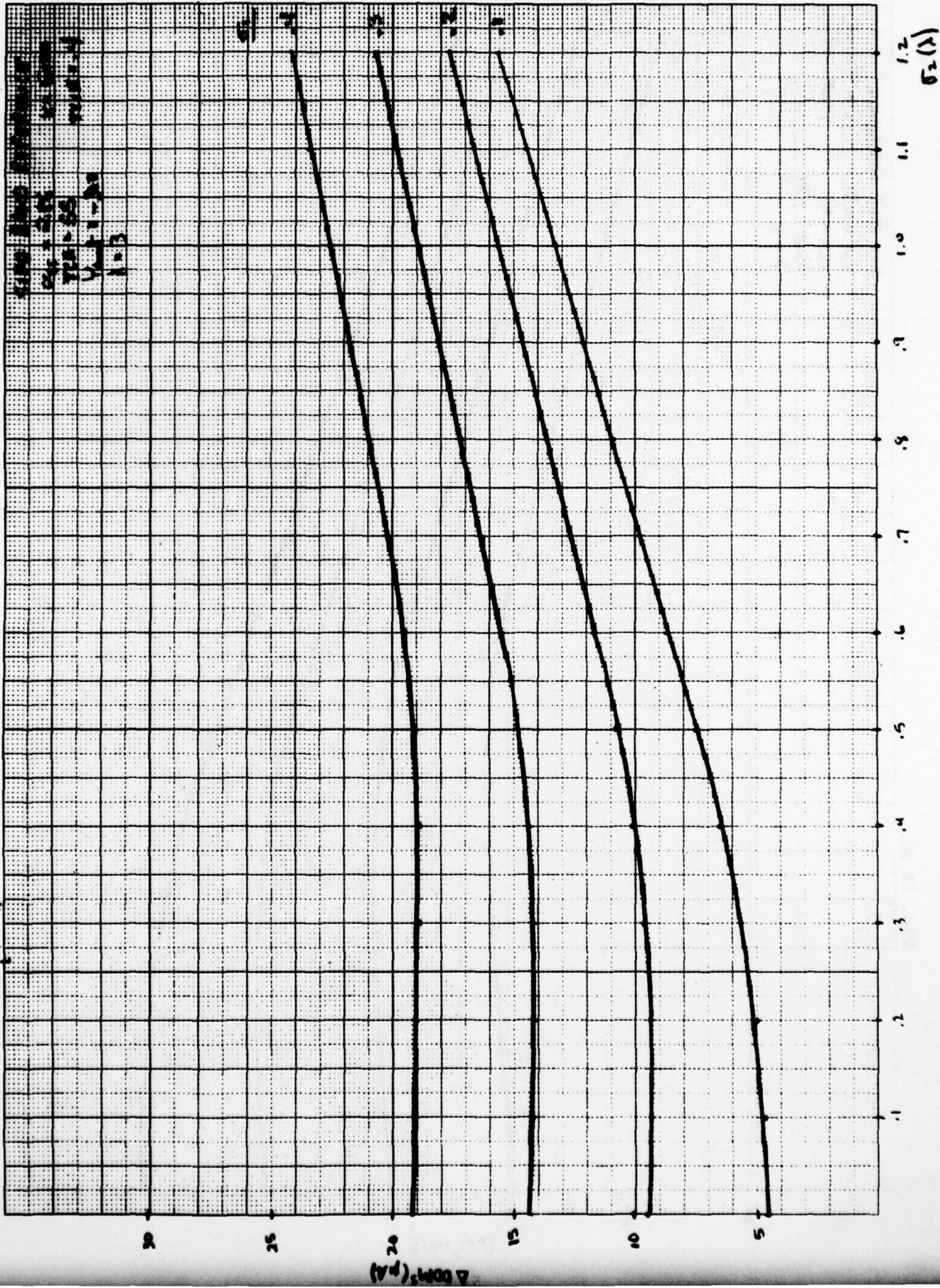


Fig. II 8e.

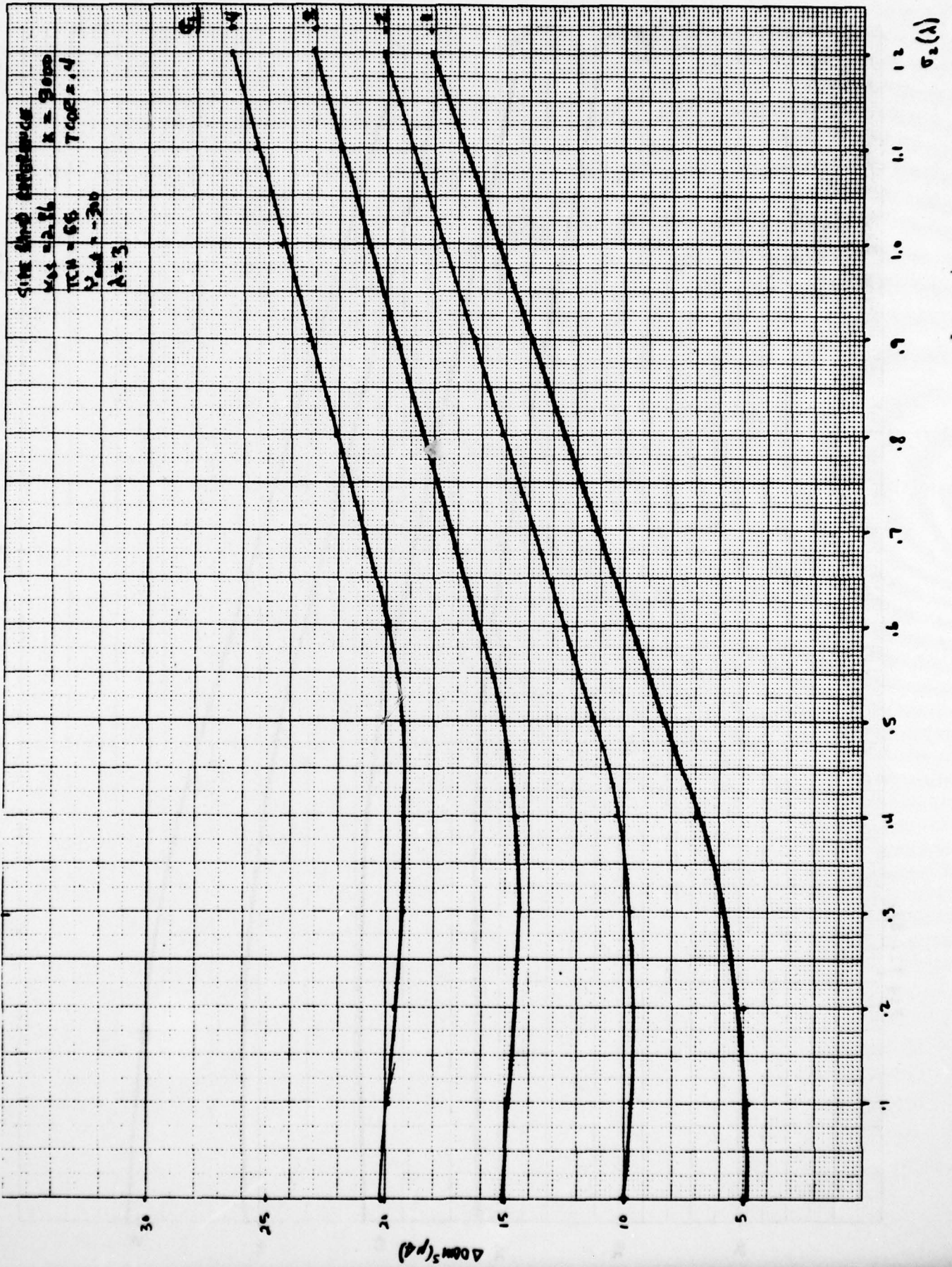


Fig. II 9

CAPTURE EFFECT FLY-INS

- 2.86° PATH
- 300' OFFSET
- .55' TCH
- FOCUSED
- STANDARD HEIGHT
- VARIABLE EDGE

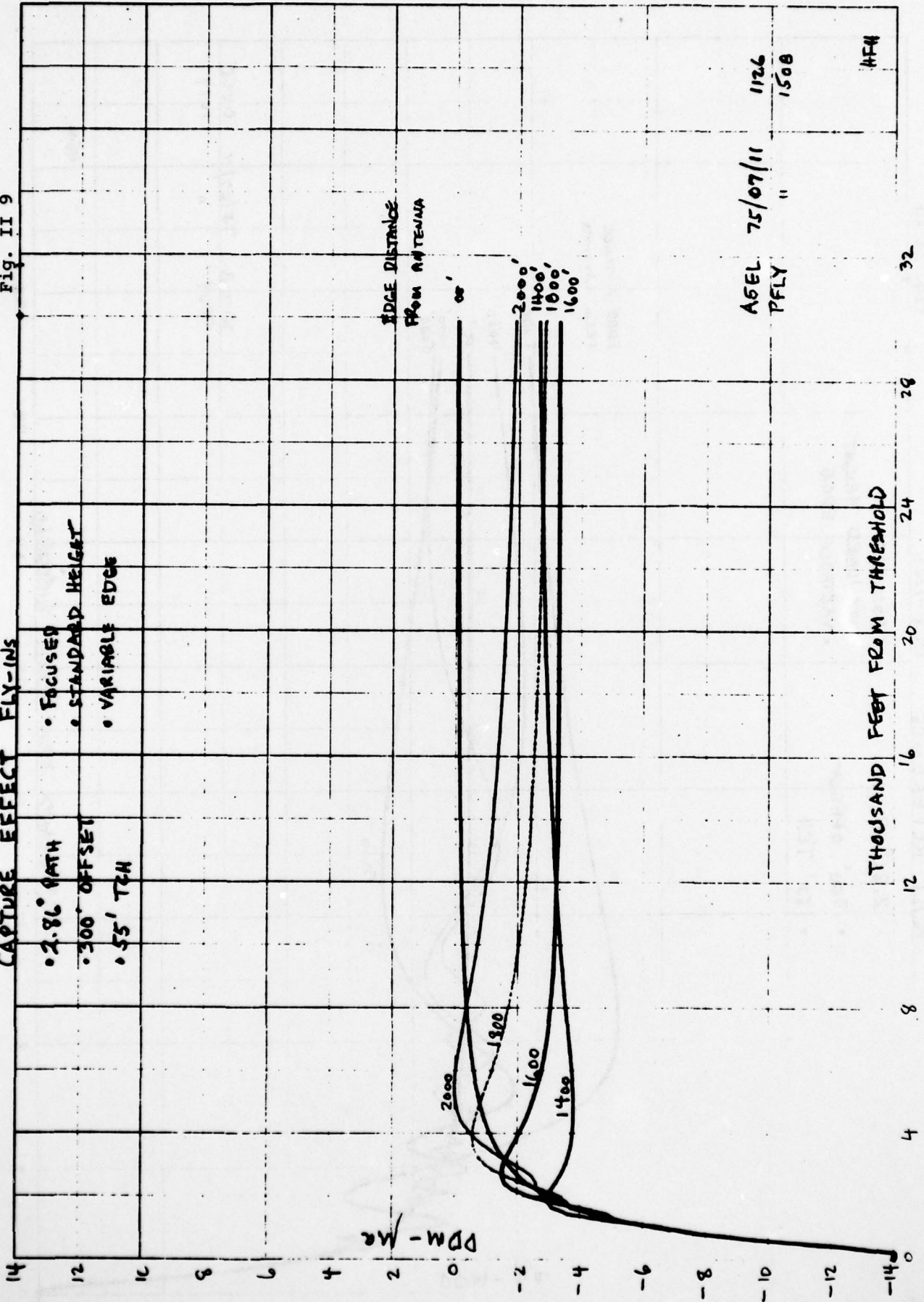


Fig. II 11

SIDEBAND REFERENCE FLY-INS

- 2.96° PATH
- 300' OFFSET
- 55' TCA
- FOCUSED
- STANDARD HEIGHT
- VARIABLE EDGE

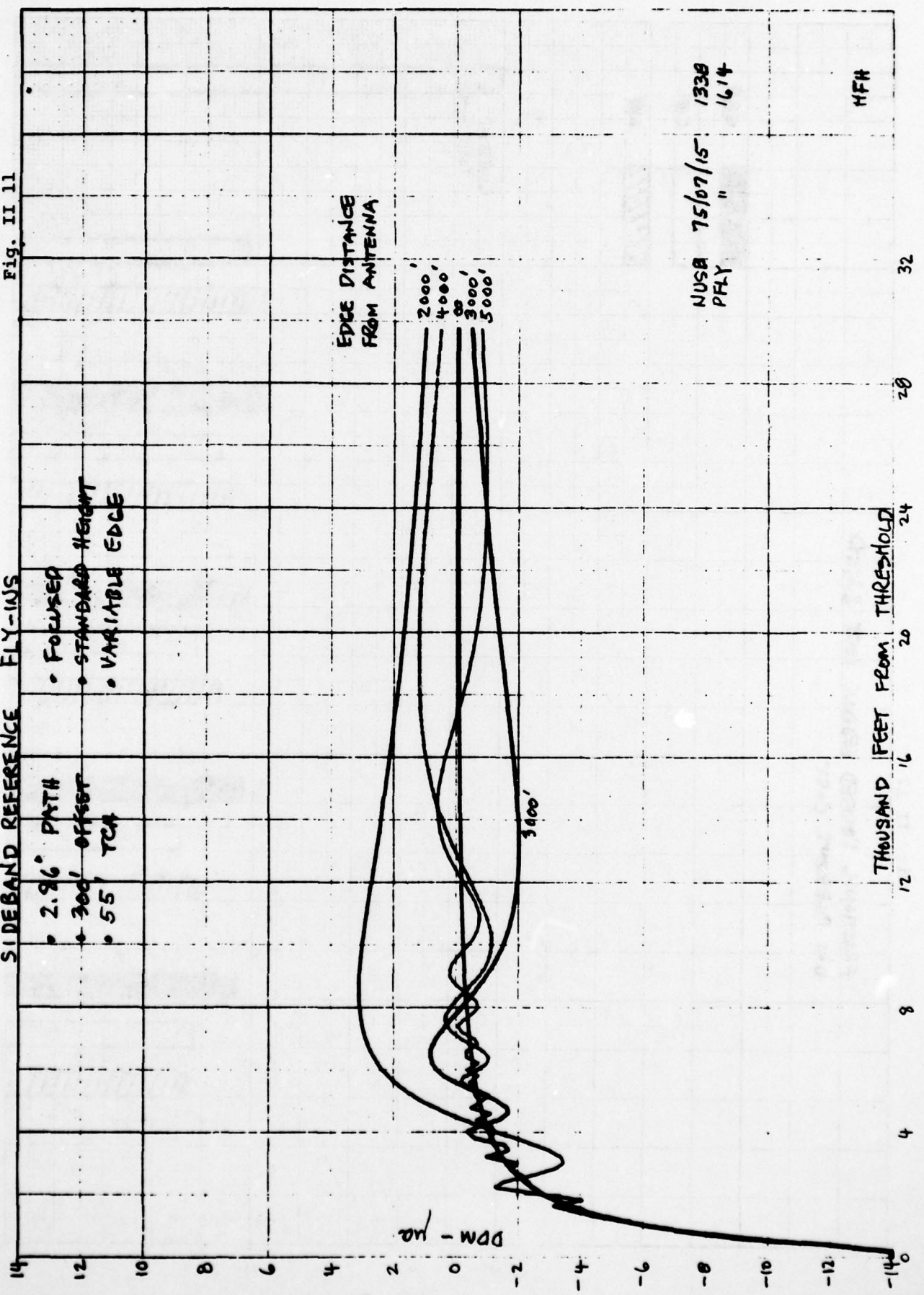
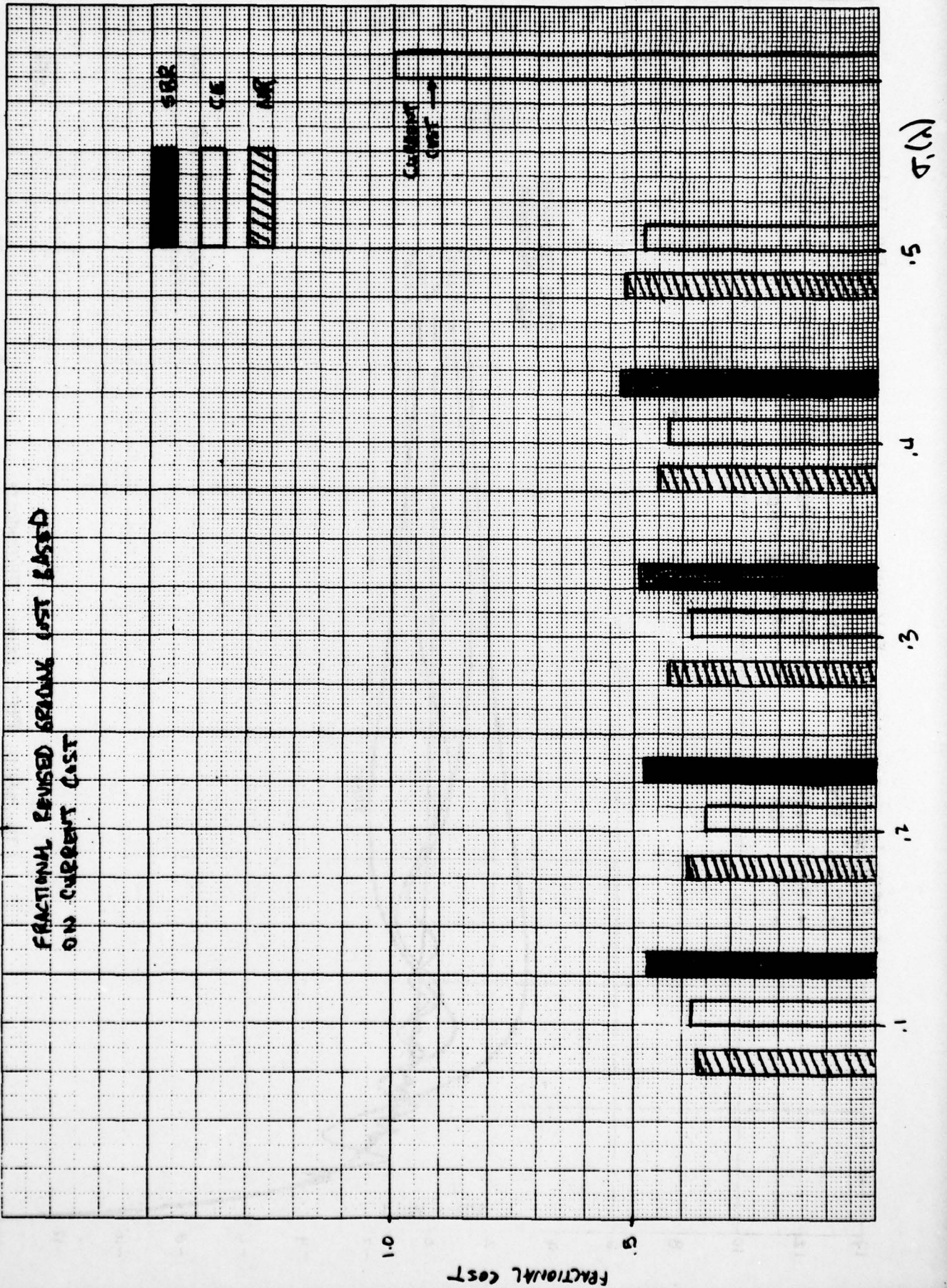


Fig. II 12

FRACTIONAL REVISED BRONK COST BASED
ON CURRENT COST



Station $\Delta DM^5 \sigma_1$	Null Reference				Capture Effect				Subband Reference					
	0.1	0.2	0.3	0.4	0.5	0.1	0.2	0.3	0.4	0.5	0.1	0.2	0.3	0.4
± 5	0.43	0.38	-	-	-	0.39	0.32	-	-	-	0.15	-	-	-
± 10	0.75	0.66	0.62	0.50	-	0.63	0.61	0.57	-	-	0.36	0.25	-	-
± 15	1.13	1.02	0.86	0.78	0.75	0.95	0.86	0.79	0.75	0.72	0.55	0.50	0.40	-
± 16	1.23	1.11	0.93	0.83	0.79	1.01	0.93	0.83	0.78	0.76	0.58	0.53	0.45	-
± 17	1.31	1.20	1.01	0.87	0.82	1.07	1.00	0.89	0.82	0.80	0.62	0.57	0.50	-
± 18	1.37	1.30	1.10	0.93	0.86	1.15	1.06	0.95	0.86	0.83	0.66	0.61	0.54	-
± 19	1.44	1.34	1.20	0.99	0.90	1.22	1.13	1.01	0.90	0.86	0.70	0.65	0.58	0.40
± 20	1.51	1.42	1.30	1.06	0.94	1.30	1.20	1.08	0.95	0.90	0.73	0.68	0.62	0.50

TABLE II-I VALUES OF ROUGHNESS $\sigma_2(\lambda)$ VERSUS $\sigma_1(\lambda)$
FOR VARIANCE IN DDM, $\Delta DDM^5(\mu A)$

ADDM ² (μA)	Null Reference		Capture Effect		Sidelobe Reference	
	Metal	Std. Earth	Metal	Std. Earth	Metal	Std. Earth
2.5	.023	.033	.018	.024	.007	.015
5.0	.035	.048	.024	.032	.012	.022
7.5	.045	.058	.028	.038	.016	.028
10.0	.052	.066	.032	.044	.020	.034
12.5	.058	.073	.036	.050	.023	.039
15.0	.062	.079	.039	.057	.025	.043
17.5	.065	.084	.042	.064	.028	.047
20.0	.068	.088	.045	.070	.030	.052
22.5	.070	.092	.048	.078	.033	.056
25.0	.073	.095	.051	.086	.036	.060
27.5	.075	.099	.055	.094	.039	.065
30.0	.078	.103	.057	.102	.041	.070

TABLE II-2 VALUES OF ROUGHNESS $\sigma_s(\lambda)$ VERSUS DDM ERROR FROM DIFFUSE REGION

σ_T	Null Reference	Capture Effect	Subband Reference
0.1	26	40	18
0.2	75	111	53
0.3	117	175	83
0.4	156	235	109
0.5	229	296	140

TABLE D-3 RADIUS OF DIFFUSE AREA (A)
VERSUS σ_T (A)